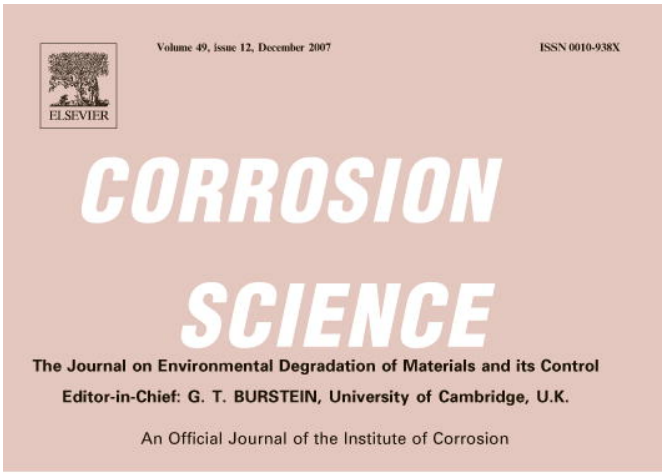

CONTENTS

G. T. Burstein	4307	Submission of manuscripts to Corrosion Science on line
Review		
S. Nešić	4308	Key issues related to modelling of internal corrosion of oil and gas pipelines – A review
Papers		
A. B. M. Mujibur Rahman, S. Kumar and A. R. Gerson	4339	Galvanic corrosion of laser weldments of AA6061 aluminium alloy
S. J. Yuan, A. M. F. Choong and S. O. Pehkonen	4352	The influence of the marine aerobic *Pseudomonas* strain on the corrosion of 70/30 Cu–Ni alloy
R. K. Singh Raman, R. Rihan and R. N. Ibrahim	4386	Role of imposed potentials in threshold for caustic cracking susceptibility (K_{SCC}): Investigations using circumferential notch tensile (CNT) testing
R. A. Castelli, P. D. Persans, W. Strohmayer and V. Parkinson	4396	Optical reflection spectroscopy of thick corrosion layers on 304 stainless steel
P. Kapsalas, M. Zervakis and P. Maravelaki-Kalaitzaki	4415	Evaluation of image segmentation approaches for non-destructive detection and quantification of corrosion damage on stonework
C. N. Panagopoulos and E. P. Georgiou	4443	The effect of hydrogen charging on the mechanical behaviour of 5083 wrought aluminum alloy
E. Blasco-Tamarit, A. Igual-Muñoz and J. García-Antón	4452	Galvanic corrosion of high alloyed austenitic stainless steel welds in LiBr systems

Contents continued on outside back cover

http://www.elsevier.com/locate/corsci

Available online at www.sciencedirect.com
ScienceDirect
Corrosion Science 49 (2007) 4308–4338
CORROSION SCIENCE
www.elsevier.com/locate/corsci

Review

Key issues related to modelling of internal corrosion of oil and gas pipelines – A review

Srdjan Nešić *

Institute for Corrosion and Multiphase Technology, Ohio University, 342 West State Street, Athens, OH 45701, USA

Received 20 December 2005; accepted 5 June 2007
Available online 14 July 2007

Abstract

The state-of-the-art in modelling of internal corrosion of oil and gas pipelines made from carbon steel is reviewed. The review covers the effects of: electrochemistry, water chemistry, formation of protective scales and scales, temperature, flow, steel, inhibition, water condensation, glycol/methanol and localized attack. Various mathematical modelling strategies are discussed.

Keywords: A. Acetic acid; A. H_2S; B. CO_2 corrosion; B. Review; B. Water wetting

Contents

1. Introduction 4309
2. The background 4311
   2.1. Electrochemistry of CO_2 corrosion 4311
      2.1.1. Anodic reaction 4311
      2.1.2. Cathodic reactions 4313
   2.2. Effect of water chemistry 4314
      2.2.1. Protective scales 4316
      2.2.2. The effect of pH 4318
      2.2.3. The effect of CO_2 partial pressure 4319

* Tel.: +1 740 593 9945; fax: +1 740 593 9949.
E-mail address: nesic@ohio.edu

0010-938X/$ - see front matter
doi:10.1016/j.corsci.2007.06.006

2.2.4. The effect of HAc 4320
2.2.5. Non-ideal behaviour 4322
2.3. The effect of temperature 4322
2.4. The effect of flow 4322
2.4.1. Multiphase flow 4324
2.5. The effect of steel type 4324
2.6. Effect of corrosion inhibition 4325
2.6.1. Corrosion inhibitors 4325
2.6.2. Corrosion inhibition by crude oil 4325
2.7. Effect of condensation 4325
2.8. Effect of glycol/methanol 4326
2.9. Localized attack 4326
3. The mathematical models 4327
3.1. Mechanistic models 4328
3.1.1. The beginnings 4328
3.1.2. Electrochemical models 4329
3.1.3. Transport based electrochemical models 4331
3.2. Semi-empirical models 4332
3.3. Empirical models 4333
4. Conclusions 4334
References 4336

1. Introduction

Building models of physico-chemical processes has many purposes. They are of help to an engineer in industry as much as to a researcher in a laboratory. Models (should) reflect a way of thinking, a way of making sense of all the accumulated information, a way of seeing how it all fits together (or does not), and last but not least are a tool to predict what may happen in the future. Models are tools that can assist engineers in making decisions related to design, operations and control.

Not all models are endless rows of complex equations. Qualitative, physico-chemical models are what we often refer to as *explanations*, and they are the hardest ones to come by. If something can be explained the rest of the modelling process is usually a mathematical exercise.

In the text below, the state-of-the-art in modelling of internal corrosion of oil and gas pipelines made from carbon steel is reviewed. This area of corrosion is often referred to simply as ''carbon dioxide corrosion'', even if it frequently involves other corrosive species such as hydrogen sulphide, organic acid, etc. The review below focuses primarily on physico-chemical modelling of sweet (CO_2) corrosion, while a discussion of sour corrosion (due to H_2S) exceed the scope of this paper. The paper reflects how much the author believes we *understand* about the complex processes underlying CO_2 corrosion taking place. A few different strategies on how this understanding can be converted into mathematical equations are outlined in the second part of the paper. Many of the details about the equations as well as most of the numerical and programming aspects of modelling are omitted and the interested reader is referred to the original publications.

Nomenclature

A/V	surface area-to-volume ratio, 1/m
b_a, b_c	anodic and cathodic Tafel slope, V/decade
c_j	concentration of species j, kmol/m^3
c_r and c_p	concentrations of reactants and products, kmol/m^3
CR	corrosion rate, mm/y
$[CO_2]_b$	bulk concentration of dissolved carbon dioxide, mol/m^3
d	droplet diameter, m
D	diffusion coefficient, m^2/s, pipe diameter, m
$D_j^{eff} = D_j^m + D_j^t$	the effective diffusion coefficient of species j, in m^2/s
D_j^m	molecular diffusion coefficient of species j, in m^2/s
D_j^t	turbulent diffusion coefficient in m^2/s
E_{rev}	reversible potential, V
F	Faraday constant (96,490 C/equiv.)
f	correction factor, constant in Frumkin model, friction factor
$[H^+]_s$, $[H^+]_b$	surface and bulk hydrogen ion concentration, mol/m^3
$[HAc]_s$, $[HAc]_b$	surface and bulk free acetic acid concentration, mol/m^3
i	current density, A/m^2
i_a	anodic current density, A/m^2
i_c	cathodic current density, A/m^2
i_{ct}	charge transfer component of the total current density, A/m^2
i_o	exchange current density, A/m^2
i_{lim}	limiting current density, A/m^2
i_{lim}^d	diffusion limiting current density, A/m^2
i_{lim}^r	chemical reaction limiting current density, A/m^2
k_m	mass transfer coefficient, m/s
k_f and k_b	forward and backward reaction rate constants
k_{hyd}^f	forward reaction rate for the CO_2 hydration reaction, 1/s
$K_{a/d}$	equilibrium constant for inhibitor adsorption/desorption
K_{hyd}	equilibrium constant for the CO_2 hydration reaction
K_{sp}	solubility limit
M	molar mass, kg/kmol
p_{CO_2}	partial pressure of carbon dioxide gas, bar
R	universal gas constant (8.3143 J/(mol K))
R_j	source or sink of species j due to chemical reactions, kmol/m^3 s
R_{FeCO_3}	precipitation rate of iron carbonate, mm/y
$Re = \rho v l/\mu$	Reynolds number
t	temperature, °C, or time, s
S	supersaturation
ST	scaling tendency
T	absolute temperature, K
v	velocity, m/s
U_c	superficial velocity of the continuous phase, m/s
V_{cor}	corrosion rate, mm/y

$We_o = \frac{\rho_o D U_c^2}{\sigma}$	Weber number
x	spatial coordinate, m
ε	porosity of the scale, water cut
$\eta = E - E_{rev}$	overpotential, V
μ	viscosity, kg/(m s)
ρ	density, kg/m^3
ρ_o	oil density, kg/m^3
ρ_μ	mixture density, kg/m^3
ζ	ratio between the thickness of the mass transfer and chemical reaction boundary layer
θ	pipe inclination, degrees

The following topics will be covered in the text below:

- Electrochemistry of CO_2 corrosion.
- CO_2 water chemistry including formation of protective scales and scales.
- Effect of temperature.
- Effect of flow.
- Effect of steel type.
- Effect of inhibition by inhibitors and crude oil.
- Effect of condensation.
- Effect of glycol/methanol.
- Localized attack.
- Mathematical modelling strategies.

2. The background

2.1. Electrochemistry of CO_2 corrosion

Aqueous CO_2 corrosion of carbon steel is an electrochemical process involving the anodic dissolution of iron and the cathodic evolution of hydrogen. The overall reaction is:

$$Fe + CO_2 + H_2O \rightarrow FeCO_3 + H_2 \quad (1)$$

The electrochemical reactions are often accompanied by the formation of scales such as $FeCO_3$ (and/or Fe_3O_4 particularly at higher temperature), which can be protective or non-protective depending on the conditions under which they are formed.

2.1.1. Anodic reaction

The anodic dissolution for iron in acid solutions:

$$Fe \rightarrow Fe^{++} + 2e^- \quad (2)$$

has been studied extensively with several multi-step mechanisms suggested to explain the various experimental results. The reaction is pH dependent in acidic solutions with a

reaction order with respect to OH^- between 1 and 2, decreasing toward 1 and 0 at pH > 4. Measured Tafel slopes are typically 30–40 mV. This subject, which is controversial with respect to the mechanism, is reviewed in detail by Drazic [1] and Lorenz and Heusler [2]. The anodic dissolution in aqueous CO_2 solutions has, until recently [3], not been the subject of detailed mechanistic studies.

The mechanism found by Bockris et al. [4] (BDD) in strong acids:

$$\begin{aligned} &Fe + H_2O \Longleftrightarrow FeOH + H^+ + e^- \\ &FeOH \overset{rds}{\rightarrow} Fe\ OH^+ + e^- \\ &FeOH^+ + H^+ \Longleftrightarrow Fe^{++} + H_2O \end{aligned} \tag{3}$$

which predicts a Tafel slope of $2RT/3F = 40$ mV at 25 °C and a reaction order with respect to OH^- equal to one, has frequently been assumed to apply in CO_2 solutions. It was overlooked that the experimental results presented by Bockris et al. [4] show that the pH dependency decreases rapidly above pH 4 and that is exactly the area of CO_2 corrosion where it was subsequently (ab)used [5–8].

Hurlen et al. [9] concluded that the active dissolution of iron appears to be little affected by CO_2 in aqueous salt solutions, but that CO_2 stimulates iron dissolution in the intermediate prepassive state. They reported a Tafel slope of ca. 30 mV at 25 °C and a first order dependency.

Gray et al. [7,8] studied the effect of pH and temperature on the mechanism of carbon steel corrosion in aqueous CO_2 solutions and their ''modelled'' Tafel constants for anodic iron dissolution increased from 50 to 120 mV in the pH range 2–10 whereas the exchange current density (i_o) values were relatively independent of pH. They also reported that the anodic polarization curve in the region near the corrosion potential was significantly increased by the presence of dissolved CO_2 at pH 6–10. It was also found that the Tafel constants for the anodic dissolution of iron derived from the study were proportional to the absolute temperature T, and that the i_o values in the presence and absence of CO_2 were proportional to $1/T$ up to 60 °C, above which temperature the dependency was substantially decreased. The latter is probably due to formation of protective iron carbonate layers which changed the kinetics of the process.

The de Waard and Milliams [5] model for aqueous CO_2 corrosion assumed that the BDD mechanism applied. They obtained similar Tafel slopes 30–40 mV in the absence and presence of CO_2 and no change in the position of the Tafel slope. Davies and Burstein [10] suggested that the formation of the complex $Fe(CO_3)_2^{2-}$ during the corrosion of iron in bicarbonate solution governs the anodic behaviour of iron in the active region.

Videm [11] found that the anodic dissolution in NaCl solution, at $p_{CO_2} = 1$ bar, in the active region had a reaction dependency with respect to OH^- equal to 1 at pH < 4.2. At higher pH values the dissolution was independent of pH. At pH > 4.3 the presence of CO_2 increased the rate of anodic dissolution and this effect was proposed to relate to the concentration of the bicarbonate ions.

In a more recent study, Nešić et al. [3] have reported that the anodic dissolution of iron is affected by the presence of CO_2. They explained that the different kinetics of iron dissolution in CO_2 solutions compared to strong acids, are due to a carbonic species acting as a chemical ligand and catalysing the dissolution of iron. This effect was independent of pH. Since H_2CO_3 and dissolved CO_2 are the only carbonic species whose concentrations do not depend on pH, and since the concentration of CO_2 is far higher of the two, it was assumed

the ligand $Fe_L = Fe–CO_2$ is formed as an adsorbed species at the electrode surface. Several detailed multi-step models were presented to explain the various findings. The following mechanism was proposed to explain the experimental results at pH > 5:

$$\begin{aligned}
&Fe + CO_2 \Longleftrightarrow Fe_L \\
&Fe_L + H_2O \Longleftrightarrow Fe_LOH_{ad} + H^+ + e^- \\
&Fe_LOH_{ad} \overset{rds}{\rightarrow} Fe_LOH^+_{ad} + e^- \\
&Fe_LOH^+_{ad} + H_2O \Longleftrightarrow Fe_L(OH)_{2ad} + H^+ \\
&Fe_L(OH)_{2ad} \Longleftrightarrow Fe_L(OH)_{2sol} \\
&Fe_L(OH)_{2sol} + 2H^+ \Longleftrightarrow Fe^{2+} + CO_2 + 2H_2O
\end{aligned} \tag{4}$$

2.1.2. Cathodic reactions

The presence of CO_2 increases the rate of corrosion of iron in aqueous solutions by increasing the rate of the hydrogen evolution reaction. In strong acids, which are completely dissociated, the rate of hydrogen evolution cannot exceed the rate at which H^+ ions can be transported to the surface from the bulk solution. In solutions with a pH > 4 this mass transfer controlled limiting current is small and the presence of H_2CO_3 enables hydrogen evolution at a much higher rate. Thus at a given pH the presence of CO_2 leads to a much higher corrosion rate than would be found in a solution of a strong acid. Despite more than three decades of intense research, it is still not known with absolute certainty whether H_2CO_3 is reduced directly (as assumed by many workers in the field) [5,7,12] or the final step in the reaction follows the dissociation of the H_2CO_3 [13]. Many have assumed that the two reactions are independent and the net cathodic current is the sum of the currents for the two reactions [7] (see Fig. 1):

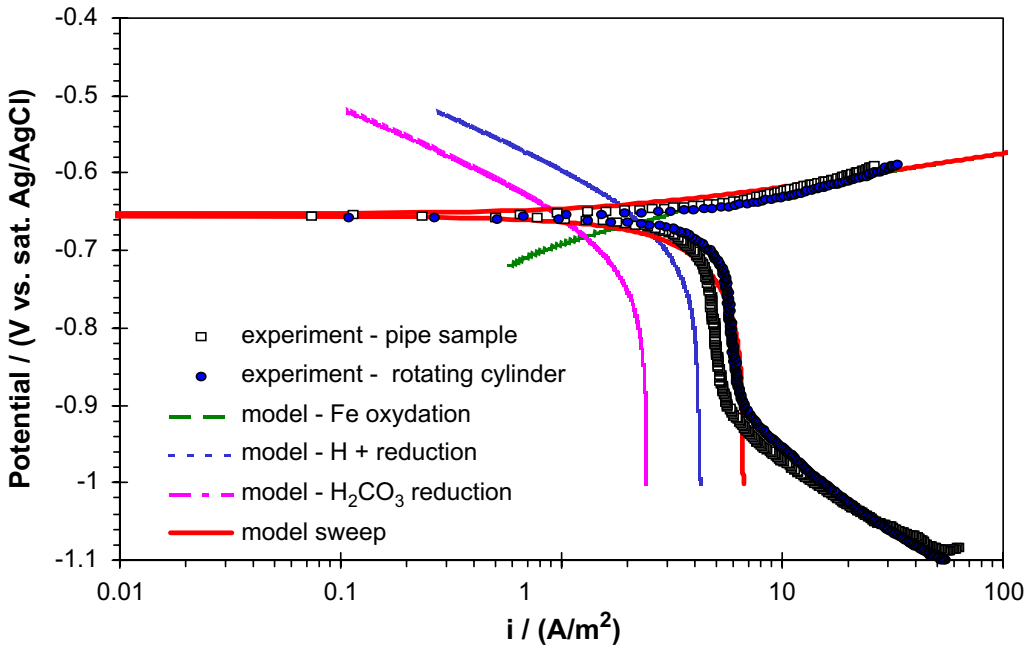

Fig. 1. Predicted and measured potentiodynamic sweeps illustrating the two cathodic reactions underlying CO_2 corrosion. Test conditions: pH 4, 20 °C, $P_{CO_2} = 1$ bar, 2 m/s, $c_{Fe^{2+}} < 2$ ppm. Model of Nešić et al. [21] was used. Experimental data taken from Nešić et al. [69].

$$2H^+ + 2e^- \rightarrow H_2 \quad (5)$$

$$2H_2CO_3 + 2e^- \rightarrow H_2 + 2HCO_3^- \quad (6)$$

The limiting currents for hydrogen evolution in aqueous CO_2 solutions do not respond to changes in the solution flow rate in a manner that would be expected for a wholly mass transfer controlled reaction, and the higher the pH the less the response to flow rate changes. This has been explained on the basis that the replenishment of the H_2CO_3 is controlled by the slow hydration of dissolved CO_2. Schmitt and Rothman [6] were the first to observe the chemical reaction component of the limiting current, suggesting a heterogeneous reaction control relating to surface adsorption. Since the effect is the same on platinum and iron, homogeneous control is now accepted [12].

Hydrogen evolution from the direct reduction of water which occurs at lower potentials becomes important [14,15] at pH > 5 and very low partial pressures of CO_2

$$2H_2O + 2e^- \rightarrow H_2 + 2OH^- \quad (7)$$

Gray et al. [8] have suggested that in CO_2 solutions at higher pH the direct reduction of the bicarbonate ion becomes important:

$$2HCO_3^- + 2e^- \rightarrow H_2 + 2CO_3^{2-} \quad (8)$$

due to the increasing concentrations of bicarbonate with increasing pH. While appealing, this reaction path for hydrogen evolution is difficult to distinguish experimentally from the other two (Eqs. (5) and (6)). Indeed it has been observed that the corrosion rates steadily decrease with pH in the range $4 < pH < 7$ while the concentration of bicarbonate ion steadily increases, bringing the significance of reaction (8) into question.

2.2. Effect of water chemistry

Probably one of the most influential parameters affecting CO_2 corrosion is the water chemistry. The speciation can vary from very simple, with only a few carbonic species present, as is the case with condensed water in gas pipelines, to very complex with numerous species found, for example, in formation water emerging together with crude oil. In the latter case the picture can be complicated further by the presence of species that partition into the water from the oil phase. In some cases the concentration of dissolved salts can be very high (>10 wt%) making the solution non-ideal. A list of typical dissolved species found in formation water is given in Table 1.

Corrosion of mild steel in oilfield brines is related to the presence of dissolved gases: CO_2 in the first place and in some instances H_2S. In many cases organic acids are present and in particular acetic acid[1] (HAc) that can aggravate the corrosion problem further, as will be discussed below. Dissolved CO_2 hydrates to form carbonic acid, which dissociates to give a hydrogen ion and a bicarbonate ion, which dissociates again to give another hydrogen ion and a carbonate ion. Similar happens with dissolved H_2S which also goes through two dissociation steps and acetic acid which dissociates in one step. A list of most common chemical reactions that need to be accounted for in brine chemistry is given in Table 2. Various salts can precipitate if their solubility is exceeded, the most important

[1] Acetic acid is commonly used as "representative" for all other water soluble organic acids which are found in oilfield brines, as its effect on CO_2 corrosion of mild steel is well understood.

Table 1
Species typically found in oilfield brines

CO_2	Dissolved carbon dioxide
H_2CO_3	Carbonic acid
HCO_3^-	Bicarbonate ion
CO_3^{2-}	Carbonate ion
H^+	Hydrogen ion
OH^-	Hydroxide ion
Fe^{2+}	Iron ion
Cl^-	Chloride ion
Na^+	Sodium ion
K^+	Potassium
Ca^{2+}	Calcium ion
Mg^{2+}	Magnesium ion
Ba^{2+}	Barium ion
Sr^{2+}	Strontium ion
CH_3COOH (HAc)	Acetic acid
CH_3COO^- (Ac^-)	Acetate ion
HSO_4^-	Bisulphate ion
SO_4^{2-}	Sulphate ion

Table 2
Chemical reactions typical for oil/gas field brines and their equilibrium constants

	Reaction	Equilibrium constant
Dissolution of carbondioxide	$CO_2(g) \Longleftrightarrow CO_2$	$K_{sol} = C_{CO_2}/P_{CO_2}$
Water dissociation	$H_2O \underset{K_{b,wa}}{\overset{K_{f,wa}}{\Longleftrightarrow}} H^+ + OH^-$	$K_{wa} = C_{H^+}C_{OH^-}$
Carbondioxide hydration	$CO_2 + H_2O \underset{K_{b,hy}}{\overset{K_{f,hv}}{\Longleftrightarrow}} H_2CO_3$	$K_{hy} = C_{H_2CO_3}/C_{CO_2}$
Carbonic acid dissociation	$H_2CO_3 \underset{K_{b,ca}}{\overset{K_{f,ca}}{\Longleftrightarrow}} H^+ + HCO_3^-$	$K_{ca} = C_{H^+}C_{HCO_3^-}/C_{H_2CO_3}$
Bicarbonate anion dissociation	$HCO_3^- \underset{K_{b,bi}}{\overset{K_{f,bi}}{\Longleftrightarrow}} H^+ + CO_3^{2-}$	$K_{bi} = C_{H^+}C_{CO_3^{2-}}/C_{HCO_3^-}$
Acetic acid dissociation	$HAc \underset{K_{b,ac}}{\overset{K_{f,ac}}{\Longleftrightarrow}} H^+ + Ac^-$	$K_{HAc} = C_{H^+}C_{Ac^-}/C_{HAc}$
Hydrogen sulphate anion dissociation	$HSO_4^- \underset{K_{b,HSO_4^-}}{\overset{K_{f,HSO_4^-}}{\Longleftrightarrow}} H^+ + SO_4^{2-}$	$K_{HSO_4^-} = C_{H^+}C_{SO_4^{2-}}/C_{HSO_4^-}$

Values for various constants are readily available elsewhere [17].

being iron carbonate $FeCO_3$, and various types of scale typically rich in calcium ($CaCO_3$, $CaSO_4$, etc.). The effect of surface scales on corrosion is discussed separately below.

Understanding brine chemistry is an important precondition for predicting CO_2 corrosion. Speciation can be determined by solving a set of equations for the chemical equilibria complemented with the electroneutrality equation. For the case of ideal (dilute) solutions, in the absence of complex formation, the set of equilibria equations to be solved is listed in Table 2. Two main scenarios can be encountered in the calculation process:

- when pH is accurately known (what is infrequent in the field but common in the lab), leading to a simple procedure where the speciation calculation is very straightforward;
- when the pH is unknown and the bicarbonate (HCO_3^-) content is known from titration (typical for the field). In the latter case the calculation is only slightly more involved as one has to solve a cubic equation to obtain the pH.

There is one important potential source of error associated with the second, indirect method of calculating the pH. Due to the fact that HAc was often not included in chemical analyses of brines, large errors in pH calculation were made when acetate concentration was mistakenly "lumped into" bicarbonate. A simple example can illustrate the point. Let us imagine that at 80 °C, 1 bar CO_2, titration analysis indicates $HCO_3^- = 0.013$ M in the brine. Back-calculation gives pH 6.3. This is a relatively high pH, which in combination with the high temperature could lead to protective iron carbonate scale formation. Actually with virtually any ferrous ion present in the brine supersaturation with respect to iron carbonate is achieved (e.g. for $Fe^{2+} = 1$ ppm, iron carbonate supersaturation is approximately 15, i.e. the amount of dissolved iron carbonate is 15 times higher then at equilibrium). Now let us assume that most of the measured bicarbonate is actually acetate ($HCO_3^- = 0.003$ M, $Ac^- = 0.010$ M). This corresponds to approximately 60 ppm of undissociated ("free") acetic acid in solution, a pretty common value for many fields. Back-calculation gives pH 5.6 which is a large discrepancy when compared to pH 6.3. The solution is now undersaturated with respect to iron carbonate and protective scales are not likely to form, i.e. much higher corrosion rates could be expected. This example clearly indicates that careful analyses, which distinguish HCO_3^- from Ac^-, are needed in order to properly calculate the pH in the field.

2.2.1. Protective scales

When the solubility of a salt is exceeded, it will precipitate what could lead to formation of a protective scale. The most common type of scale encountered in CO_2 corrosion is iron carbonate.

$$Fe^{2+} + CO_3^{2-} \Rightarrow FeCO_3 \tag{9}$$

When iron carbonate precipitates at the steel surface, it can slow down the corrosion process by:

- presenting a diffusion barrier for the species involved in the corrosion process;
- covering (inhibiting) a portion of the steel surface.

Iron carbonate scale growth and its protectiveness depend primarily (but not exclusively) on the precipitation rate. As the steel surface corrodes under the scale, corrosion continuously undermines the scale. As voids are created, they are filled up by the ongoing precipitation, etc. When the rate of precipitation at the steel surface exceeds the rate of corrosion (scale undermining) dense protective scales form–sometimes very thin ($\sim$1 μm) but still protective. Vice versa, when the corrosion process undermines the newly formed scale faster than precipitation can fill in the voids, a porous and unprotective scale forms - which can be sometimes very thick ($\sim$100 μm) and still unprotective.

There are many factors which affect formation of iron carbonate scales. The most important one is water chemistry, discussed below. In order to obtain appreciable levels of precipitation, supersaturation with respect to iron carbonate has to be exceeded. At room temperature, the process of precipitation is very slow and unprotective scales are usually obtained, even at very high supersaturations. Conversely, at high temperature (e.g. >60 °C) precipitation proceeds rapidly and dense and very protective scales can be formed even at low supersaturation. Actually, high supersaturation cannot be sustained

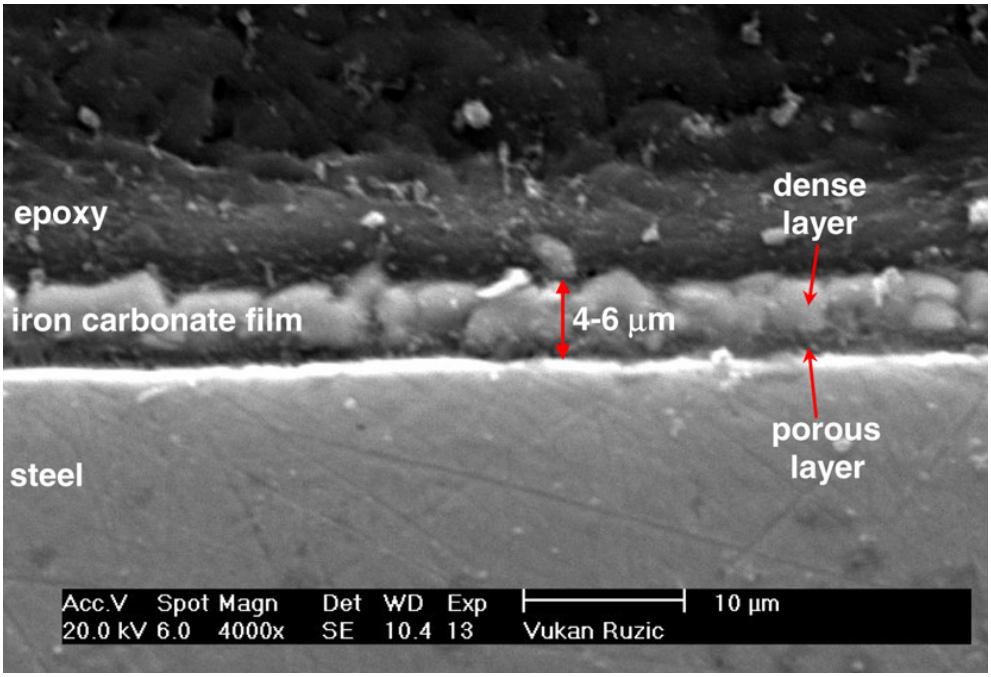

Fig. 2. SEM image of a cross section of a steel specimen including an iron carbonate scale. Exposed for 10 h at $T = 80$ °C, pH 6.6, $P_{CO_2} = 0.54$ bar, $c_{Fe^{2+}} = 250$ ppm, $v = 1$ m/s. The corrosion rate history is shown in Fig. 3. Taken from Nešić and Lee [53].

for long at high temperature as the accelerated precipitation process will tend to rapidly return the solution to thermodynamic equilibrium.

An example of an iron carbonate protective scale is shown in Fig. 2. A dense scale is seen 4–6 μm in thickness. The corresponding corrosion rate history is shown in Fig. 3. Under high supersaturation the corrosion rate was reduced rapidly as protective iron carbonate scales formed.

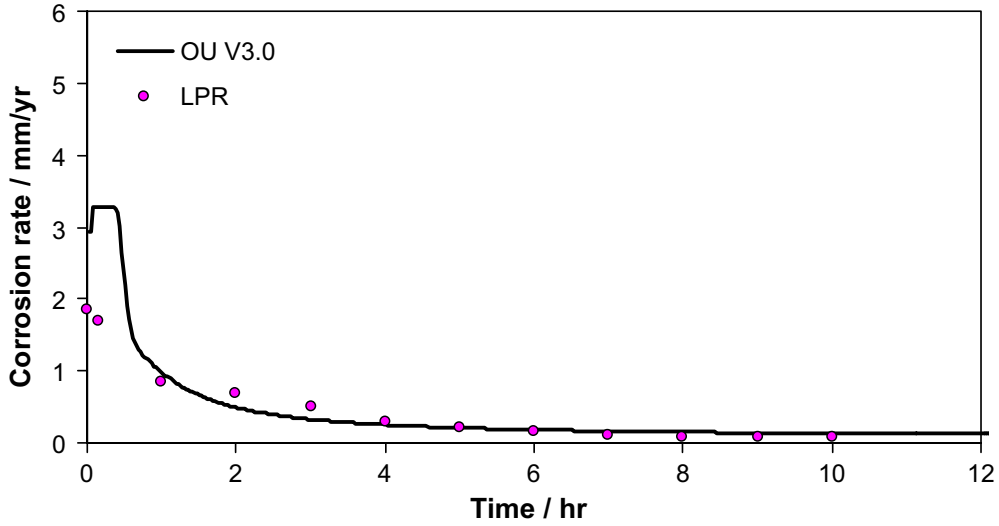

Fig. 3. Predicted (line) and experimentally measured (points) corrosion rate history showing the effect of protective scale formation. Test conditions: 80°C, pH 6.6, $P_{CO_2} = 0.54$ bar, $c_{Fe^{2+}} = 250$ ppm, $v = 1$ m/s. Data taken from Nešić and Lee [53]. SEM image of the corroded steel surface cross section shown in Fig. 2. Corrosion rates were measured by linear polarization resistance OU V 3.0 is the model of Nešić et al. [21].

Other salts can precipitate to form scales which may affect the corrosion rate. A broader analysis of general scaling and factors that affect it is beyond the scope of the present review.

2.2.2. The effect of pH

It was shown previously both experimentally and computationally [16] that pH has a strong influence on the corrosion rate. Typical pH in CO_2 saturated condensed water is about pH 4 or somewhat less. In buffered brines, one frequently encounters $5 < pH < 7$. At pH 4 or below, direct reduction of H^+ ions, Eq. (5), is important particularly at lower partial pressure of CO_2 and the pH has a direct effect on the corrosion rate (see Fig. 4).

However, the most important effect of pH is indirect and relates to how pH changes conditions for formation of iron carbonate scales. High pH results in a decreased solubility of iron carbonate and leads to an increased precipitation rate and higher scaling tendency. To illustrate this, the experimental results from Chokshi et al. [18] for various pH and supersaturations are shown in Fig. 5. At lower supersaturations obtained at pH6 the corrosion rate does not change much with time, even if some iron carbonate precipitation occurs, reflecting the fact that a relatively porous, detached and unprotective scale is formed. The higher pH6.6 results in higher supersaturation, faster precipitation and formation of more protective scales, reflected by a rapid decrease of the corrosion rate with time.

There are other indirect effects of pH, for example: the ratio of Ac^-/HAc increases with pH making the acetic acid less of a corrosion problem, high pH leads to formation of other types of scales, etc. By almost all accounts, higher pH leads to a reduction of the corrosion rate, making the "pH stabilization" (meaning pH increase) technique an attractive way of managing CO_2 corrosion. The drawback of this technique is that it can lead to excessive scaling and can be rarely used with formation water systems.

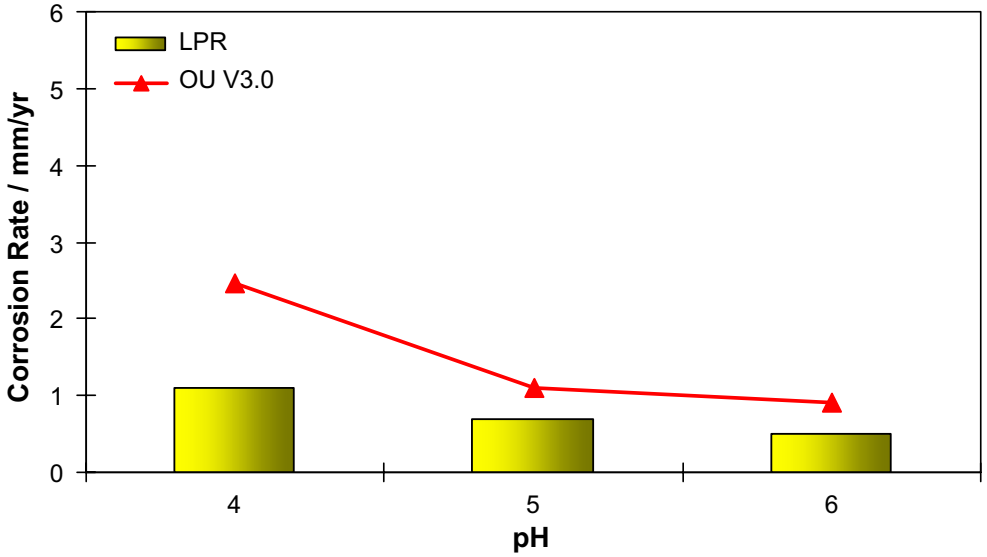

Fig. 4. Predicted and experimentally measured corrosion rates showing the effect of pH in the absence of iron carbonate scales. Test conditions: 20 °C, $P_{CO_2} = 1$ bar, 1 m/s, $c_{Fe^{2+}} < 2$ ppm. Model of Nešić et al. [21] was used. Experimental data taken from Nešić et al. [69].

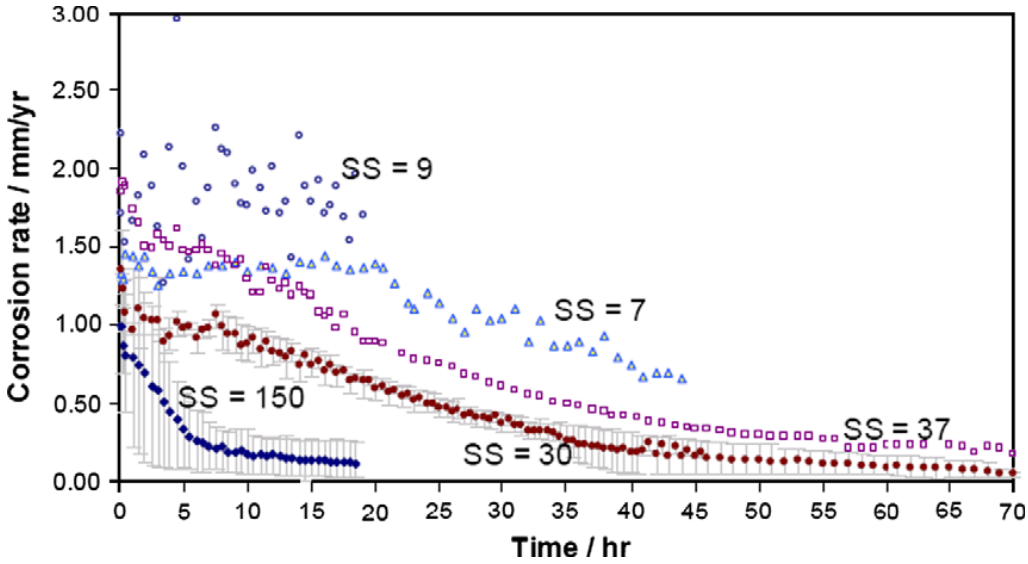

Fig. 5. Effect of iron carbonate supersaturation SS on corrosion rate obtained at a range of pH 6.0–pH 6.6, for 5 ppm $< c_{Fe^{2+}} <$ 50 ppm at $T = 80$ °C, under stagnant conditions. Error bars represent minimum and maximum values obtained in repeated experiments. Data taken from Chokshi et al. [18].

2.2.3. The effect of CO_2 partial pressure

In the case of scale-free CO_2 corrosion, an increase of CO_2 partial pressure (P_{CO_2}) typically leads to an increase in the corrosion rate. The commonly accepted explanation is that with P_{CO_2} the concentration of H_2CO_3 increases and accelerates the cathodic reaction, Eq. (6), and ultimately the corrosion rate. The effect of P_{CO_2} is illustrated in Fig. 6. However, when other conditions are favourable for formation of iron carbonate scales, increased (P_{CO_2}) can have a beneficial effect. At a high pH, higher P_{CO_2} leads to an increase

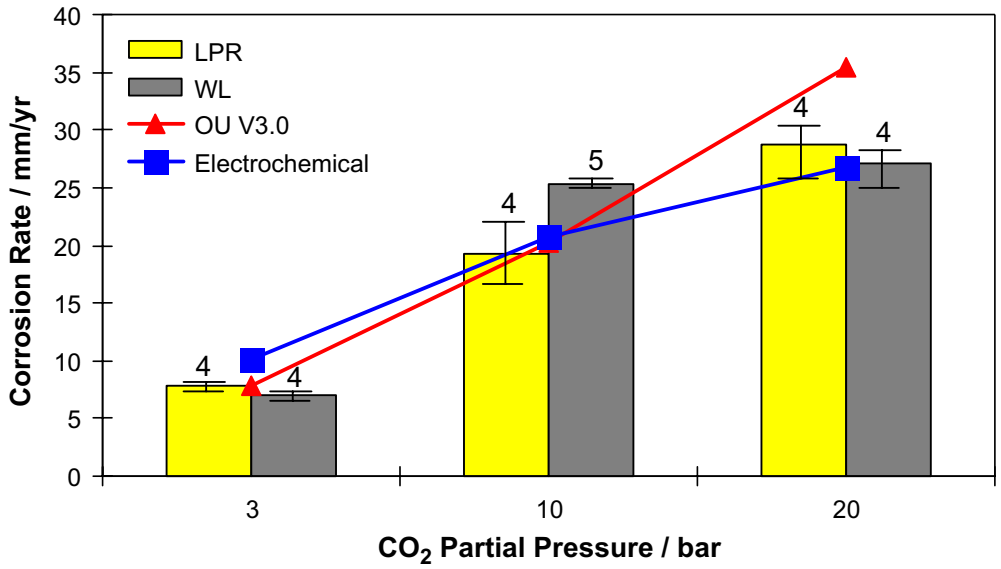

Fig. 6. Predicted and experimentally measured corrosion rates showing the effect of CO_2 partial pressure P_{CO_2}. Test conditions: 60 °C, pH5, 1 m/s. Data taken from Wang et al. [26]. Corrosion rates were measured both by linear polarization resistance (LPR) and weight loss (WL). Error bars denote maximum and minimum values and the figure above the bars is the number of repeated experiments. OU V 3.0 is the model of Nešić et al. [21], electrochemical model comes from George et al. [28].

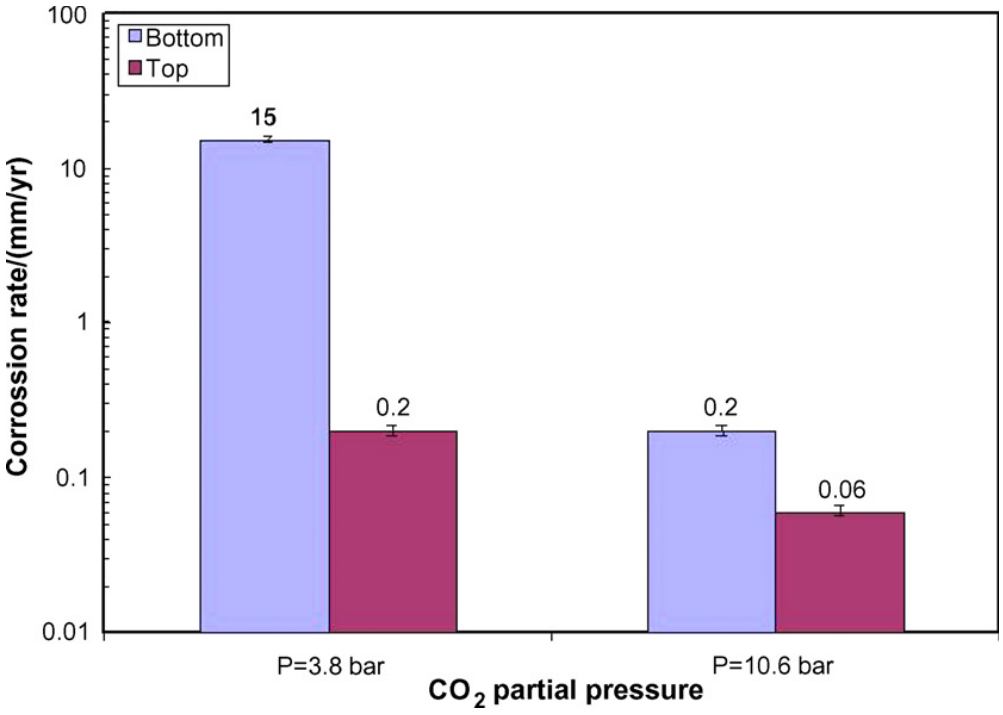

Fig. 7. Experimental measurements of the corrosion rate at the top and bottom of the pipe in multiphase stratified flow showing the effect of CO_2 partial pressure, P_{CO_2} on formation of iron carbonate scale. Test conditions: 90 °C, $V_{sg} = 10$ m/s, $V_{sl} = 0.1$ m/s. Data taken from Sun and Nešić [43].

in bicarbonate and carbonate ion concentration and a higher supersaturation, which accelerates precipitation and scale formation. The effect of P_{CO_2} on the corrosion rate in the presence of iron carbonate precipitation is illustrated in Fig. 7 where in stratified flow corrosion rate is reduced both at top and bottom of the pipe with the increase partial pressure of CO_2.

2.2.4. The effect of HAc

HAc is a weak acid, however it is stronger than carbonic acid (pK_a 4.76 vs 6.35 at 25 °C), and it is the main source of hydrogen ions when the two acid concentrations are similar. Some understanding of the role of HAc in CO_2 corrosion comes from field experience as related to the so-called Top-of-Line-Corrosion (TLC) [22]. Hedges and McVeigh [23] reported a mild increase in the cathodic reaction in the presence of HAc although their results were not fully conclusive. Garsany et al. [24] published work using voltammetry to study the effect of acetate ions on the rates and mechanisms of corrosion using a rotating disc electrode (RDE) on scale-free surfaces. Their voltammograms show two waves, which are attributed to hydrogen ion reduction (Eq. (5)) and a new cathodic reaction – HAc reduction (Fig. 8):

$$2HAc + 2e^- \rightarrow H_2 + 2Ac^- \tag{10}$$

They argue that since HAc dissociation can occur very quickly it is not possible to distinguish the reduction of hydrogen ions from direct HAc reduction at the electrode surface. Sun et al. [25] published work using potentiodynamic sweeps to study the effect of HAc on the cathodic and anodic reactions using a rotating cylinder electrode (RCE) finding that the predominant effect was cathodic. Wang et al. [26] and George et al. [27] have

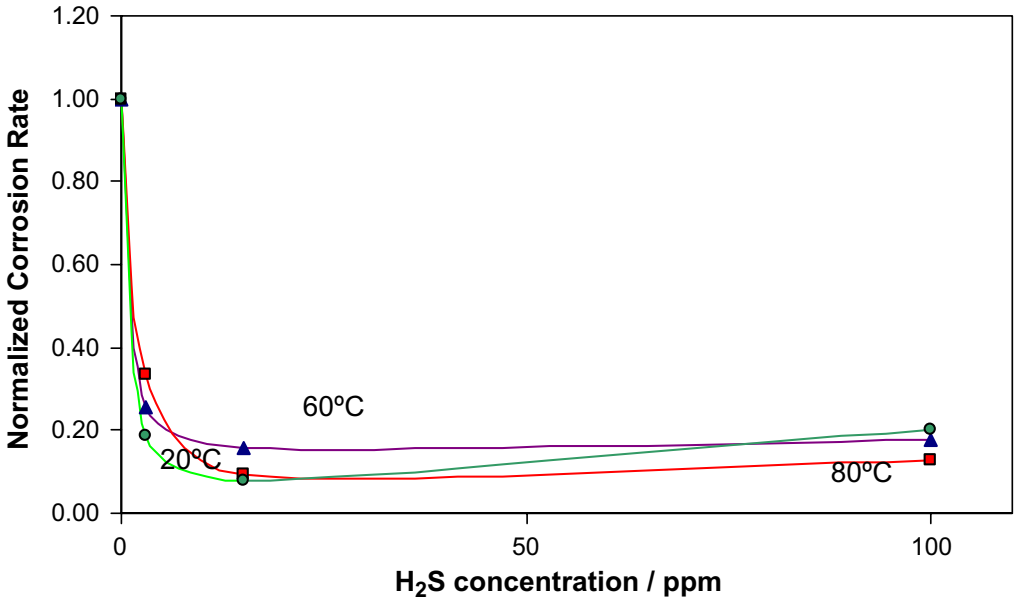

Fig. 8. Effect of low concentrations of H_2S on the CO_2 corrosion rate; ppm refers to the H_2S concentration in the gas phase. Data taken from Lee and Nešić [70].

recently published an extensive study of HAc corrosion and concluded that HAc is particularly harmful in its undissociated state. George et al. [28] have proposed models of CO_2/HAc corrosion showing the strong influence of velocity on the HAc contribution to the overall corrosion reaction. The effect of HAc is particularly pronounced at higher temperatures and low pH when the abundance of undissociated HAc can increase the CO_2 corrosion rate dramatically as seen in Fig. 9.

Theoretically solid iron acetate could precipitate via:

$$Fe^{2+} + 2Ac^{-} \Rightarrow Fe(Ac)_2 \tag{11}$$

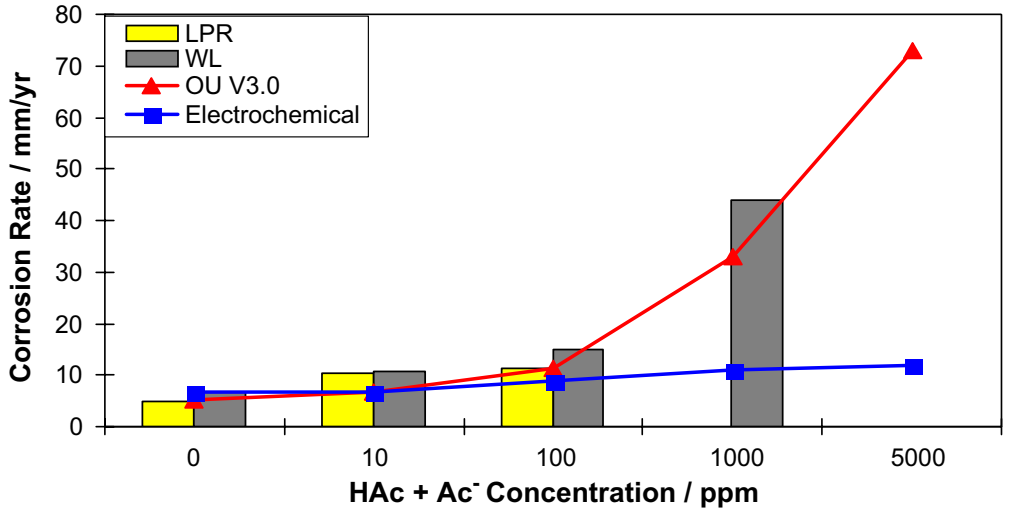

Fig. 9. Predicted and experimentally measured corrosion rates showing the effect of acetic acid. Test conditions: 60 °C, pH 4, 0.5 m/s. Data taken from George et al. [28]. Corrosion rates were measured both by linear polarization resistance (LPR) and weight loss (WL). OU V 3.0 is the model of Nešić et al. [21]. Electrochemical model comes from George et al. [28].

however, iron acetate's solubility is so much higher than iron carbonate's, that protective scale formation by iron acetate does not readily occur. It has been speculated that the presence of organic acids impairs the protectiveness of iron carbonate films, however a recent detailed study has clearly proven that this could be related to a reduction in pH in the presence of organic acids and possibly to a scale undermining effect [29]. There is no evidence that organic acids change the solubility of iron carbonate, however, this work is still ongoing and publication of the latest results is expected in the near future.

2.2.5. Non-ideal behaviour

In many cases produced water has a very high dissolved solids content (>10 wt%). At such high concentrations, the infinite dilution theory does not hold and corrections need to be made to account for solution non-ideality. A simple way to account for the effect on non-ideal homogenous water chemistry is to correct the equilibrium constants described in Table 2, by using the concept of ionic strength. This approach seems to work well only for moderately concentrated solution (up to a few wt% of dissolved solids). For more concentrated solutions a more accurate way is to use activity coefficients as described by Anderko et al. [44].

The effect of concentrated solutions on heterogeneous reactions such as precipitation of iron carbonate and other scales is still largely unknown. Furthermore, it is unclear how the highly concentrated solutions affect surface electrochemistry. Field experience suggests that corrosion rates can be dramatically reduced in very concentrated brines, nevertheless a more systematic study is needed.

At very high total pressure the gas/liquid equilibria cannot be accounted for by Henry's law. A simple correction can be made by using a fugacity coefficient which accounts for non-ideality of the CO_2/natural gas mixture [32] and can be obtained by solving the equation of state for the gas mixture.

2.3. The effect of temperature

Temperature accelerates all the processes involved in corrosion: electrochemical, chemical, transport, etc. One would expect then that the corrosion rate steadily increases with temperature, and this is the case at low pH when precipitation of iron carbonate or other protective scales does not occur. An example is shown in Fig. 10. The situation changes markedly when solubility of iron carbonate (or another salt) is exceeded, typically at a higher pH. In that case, increased temperature accelerates rapidly the kinetics of precipitation and protective scale formation, decreasing the corrosion rate. The peak in the corrosion rate is usually seen between 60 °C and 80 °C depending on water chemistry and flow conditions. Many of empirical models are built to mimic this behaviour and some are discussed below.

2.4. The effect of flow

There are two main ways in which flow may affect CO_2 corrosion which can be distinguished based on whether or not other conditions are conducive to protective scale formation or not.

- In the case of corrosion where protective scales do not form (typically at low pH as found in condensed water and in the absence of inhibitors), the main role of turbulent

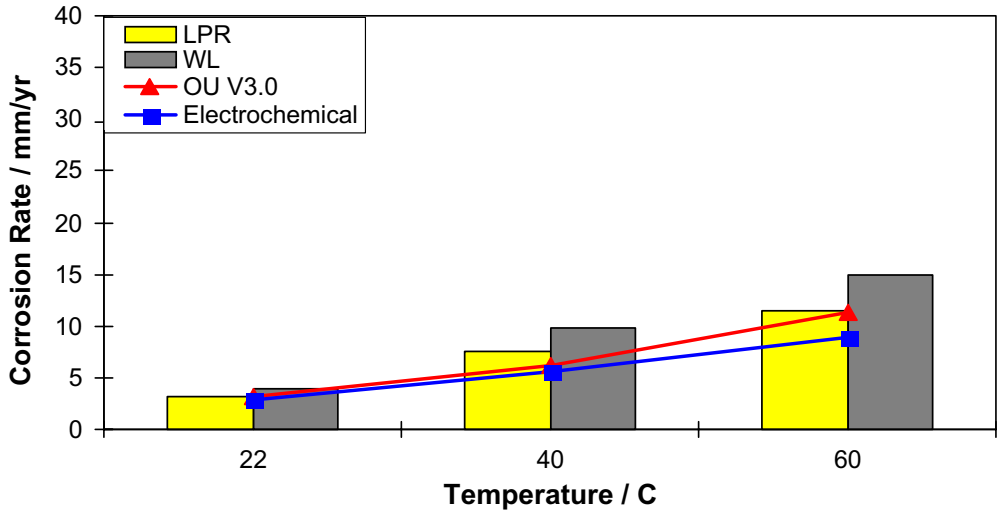

Fig. 10. Predicted and experimentally measured corrosion rates showing the effect of temperature. Test conditions: pH 4, $P_{CO_2} = 1$ bar, $c_{Fe^{2+}} < 5$ ppm, 100 ppm acetic species ($HAc + Ac^-$) $v = 0.5$ m/s. Data taken from Wang et al. [26]. Corrosion rates were measured both by linear polarization resistance (LPR) and weight loss (WL). OU V 3.0 is the model of Nešić et al. [21]. Electrochemical model comes from George et al. [28].

flow is to enhance transport of species towards and away from the metal surface. This may lead to an increase in the corrosion rate as illustrated in Fig. 11.

- Conversely, when protective iron carbonate scales form (typically at higher pH in produced water) or when inhibitor films are present on the steel surface, the above-mentioned effect of flow becomes insignificant as the main resistance to corrosion is now in the surface scale or inhibitor film. In this case, the effect of flow is to interfere with formation of surface scales/films or to remove them once they are in place, leading to an increased corrosion rate.

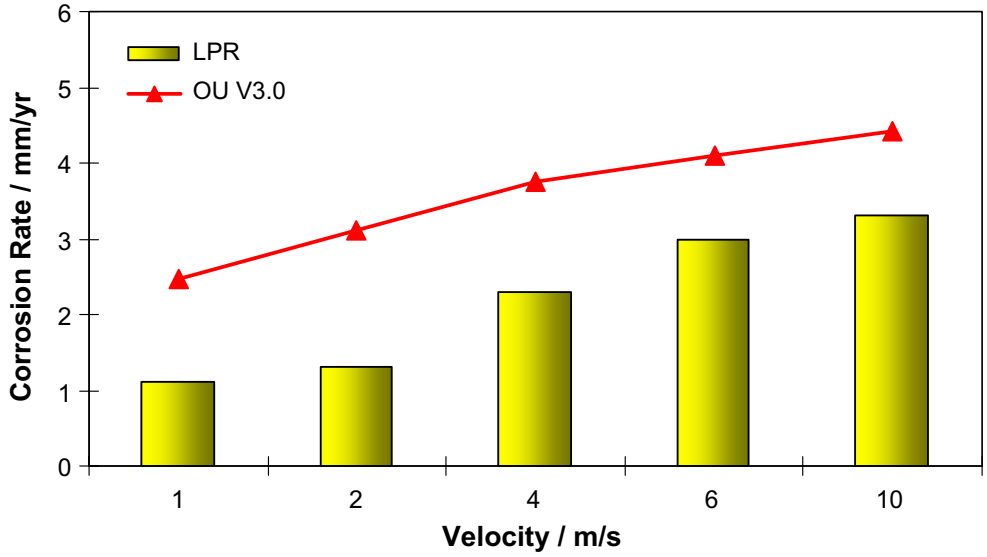

Fig. 11. Predicted and experimentally measured corrosion rates showing the effect of velocity in the absence of iron carbonate scales. Test conditions: 20 °C, $P_{CO_2} = 1$ bar, $c_{Fe^{2+}} < 2$ ppm. Model of Nešić et al. [21] was used. Experimental data taken from Nešić et al. [69].

The two flow accelerated corrosion effects discussed above are frequently aggravated by flow disturbances such as valves, constrictions, expansions, bends, etc. where local increases of near-wall turbulence and wall-shear stress are seen. In addition, multiphase flow, and in particular unsteady slug flow, can lead to significant short lived fluctuations in the wall-shear stress which can remove a protective surface scale of iron carbonate or affect the inhibitor film. Flow can lead to onset of localized attack given the "right" set of circumstances as discussed in a separate heading below.

2.4.1. Multiphase flow

One of the more complex problems is the effect of multiphase flow on CO_2 corrosion since many of the pipelines and flowlines carrying oil and gas are operating under two- or three-phase flow conditions. Different flow patterns can be found most common being: *stratified*, *slug* and *annular* flow. In the liquid phase, water and oil can flow separated or mixed with either phase being continuous with the other flowing as a dispersed phase. Different flow patterns lead to a variety of steel surface wetting mechanisms which greatly affect corrosion.

In the absence of protective scales multiphase flow can lead to very high fluctuating mass transfer rates (particularly in slug flow) which, in turn, can affect corrosion. Associated with this are even larger fluctuations of the surface shear stress which can lead to removal of protective scale and/or inhibitors. Pots [30] has proposed that the mass transfer rate in multiphase flow can be modelled by using a standard multiphase flow simulator coupled with a single-phase flow mass transfer correlation and the hydraulic diameter concept. Jepson et al. [31] suggested that the Froude number is important for characterizing the effect of multiphase flow on CO_2 corrosion, particularly in slug flow. Recently, Nešić et al. [21] have shown an integrated CO_2 corrosion/multiphase flow model which enables:

- flow pattern prediction;
- calculation of the associated hydrodynamic properties relevant for corrosion, such as: water layer velocity, thickness, etc.;
- prediction of water entrainment/wetting.

How the flow regime is actually predicted and how the hydrodynamic properties affect the corrosion rate is a topic that exceeds the scope of this paper with the details found elsewhere [21].

2.5. The effect of steel type

Most of the studies of CO_2 corrosion focus on a single mild steel: de Waard et al. [33] looked at the normalised DIN St52 steel. Nešić et al. [15] have studied predominantly the X65 low carbon steel, while the model of Gray et al. [8] was based on experiments with the production casing steel.

Nešić et al. [15], in their electrochemical model, have identified exchange current densities for iron dissolution which differed an order of magnitude for two different mild steels: X65 and St52. To account for the effect of steel, de Waard et al. [33] grouped all the tested steels in two categories: (a) normalised steels and (b) quenched and tempered steels, finding a different set of model constants for each group which improved the correlation with the experimental data.

All the above applies to the CO_2 corrosion of "bare" steel surfaces. The effect of steel composition on protective scale formation, mesa attack and adsorption of inhibitors is even more complicated. For example, it is known that a high Cr content can be beneficial for formation of protective scales but detrimental for performance of certain corrosion inhibitors. Obviously, this is an area where new research efforts are needed.

2.6. Effect of corrosion inhibition

The two most common sources of corrosion inhibition need to be considered:

(a) inhibition by addition of corrosion inhibitors and
(b) inhibition by components present in the crude oil.

2.6.1. Corrosion inhibitors

Describing the effect of corrosion inhibitors is not a straightforward task. There is a plethora of approaches in the open literature, varying from the use of simple *inhibitor factors* and *inhibition efficiencies* to the application of complicated *molecular modelling* techniques to describe inhibitor interactions with the steel surface and iron carbonate scale. A middle-of-the-road approach is based on the assumption that corrosion protection is achieved by *surface coverage*, i.e. that the inhibitor adsorbs onto the steel surface and slows down one or more electrochemical reactions. The degree of protection is assumed to be directly proportional to the fraction of the steel surface covered by the inhibitor. In this type of model one needs to establish a relationship between the surface coverage θ and the inhibitor concentration in the solution c_{inh}. This is most commonly done by the use of adsorption isotherms. It has been shown [34] that the Frumkin isotherm can be successfully used to model the degree of protection offered by the inhibitor.

2.6.2. Corrosion inhibition by crude oil

It has been known for a while that CO_2 corrosion rates seen in the field in the presence of crude oil are much lower then those obtained in laboratory conditions where crude oil was not used or synthetic crude oil was used. One can identify two main effects of crude oil on the CO_2 corrosion rate.

The first is a *wettability* effect and relates to a hydrodynamic condition where crude oil entrains the water and prevents it from wetting the steel surface (continuously or intermittently). This effect and its modelling are discussed in detail by Cai et al. [38].

The second effect is *corrosion inhibition* by certain components of the crude oil that reach the steel surface either by direct contact or by first partitioning into the water phase. Little is known about the nature and the effectiveness of these components which inhibit corrosion. In a recent detailed study [35–37] on the subject, the degree of inhibition was quantitatively related to the chemical composition of the crude oil and specifically to the concentration of saturates, aromatics, resins, asphaltenes, nitrogen and sulphur.

2.7. Effect of condensation

When transporting natural gas, due to cooling of the fluid, condensation of water vapour occurs on the internal pipe wall. The condensed water is pure and, due to dissolved

CO_2, has typically a pH < 4. This leads to the so-called *top-of-the-line corrosion* (TLC) scenario. If the rate of condensation is high, plenty of acidic water flows down the internal pipe walls leading to a very corrosive situation. If the condensation rate is low, the water film is not renewed and flows down very slowly and the corrosion process can release enough Fe^{2+} to raise the local pH and saturate the solution, leading to formation of protective iron carbonate scale. The scale is often protective, however incidents of localized attack in TLC were reported [22]. Either way, the stratified or stratified-wavy flow regime, typical for TLC, does not lead to a good opportunity for inhibitors to reach the upper portion of the internal pipe wall and protect it. A very limited range of corrosion management options for TLC exists.

To qualitatively and quantitatively describe the phenomenon of corrosion occurring at the top of the line, a deep insight into the combined effect of the chemistry, hydrodynamics, thermodynamics, and heat and mass transfer in the condensed water is needed. A full description exceeds the scope of this review, and the interested reader is directed to see some recent articles published on this topic [22,39].

2.8. Effect of glycol/methanol

Glycol and methanol are often added to flowing systems in order to prevent hydrates from forming. The quantities are often significant (50% of total liquid phase is not unusual). In the very few studies available it has been assumed that the main "inhibitive" effect of glycol/methanol on corrosion comes from dilution of the water phase, which leads to a decreased activity of water. However, there are many unanswered questions such as the changes in mechanisms of CO_2 corrosion in water/glycol mixtures which have yet to be discovered.

2.9. Localized attack

As illustrated above, significant progress has been achieved in understanding uniform CO_2 corrosion, without or with protective scales, and hence some successful uniform corrosion models have been built and will be discussed below. However, much less attention has been given to localized CO_2 corrosion and it is still not well understood. In a handful of recent studies, flow has been proposed as the main factor triggering localized attack. For example, Gunaltun [40] proposed a localized corrosion prediction model which applies a turbulence factor to modify a general corrosion rate prediction. Schmitt et al. [41] developed a probabilistic model for the prediction of flow induced localized corrosion. It is known that there are other environmental factors, such as pH, temperature, partial pressure of CO_2, etc. that contribute to occurrence of localized attack on carbon steel, and therefore a more general model that could take this into account needs to be put forward.

Recently, a number of independent studies [42,43] have suggested that localized attack can occur when the conditions are such that partially protective scales form. It is well known that when fully protective scales form, low corrosion rates are obtained and vice versa when no protective scales form a high rate of general corrosion is seen. It is when the corrosive environment is in between, in the so-called "grey zone", that localized attack is initiated due to the stochastic nature of the processes underlying corrosion. There are many hydrodynamic, (electro)chemical and metallurgical parameter combinations that fall

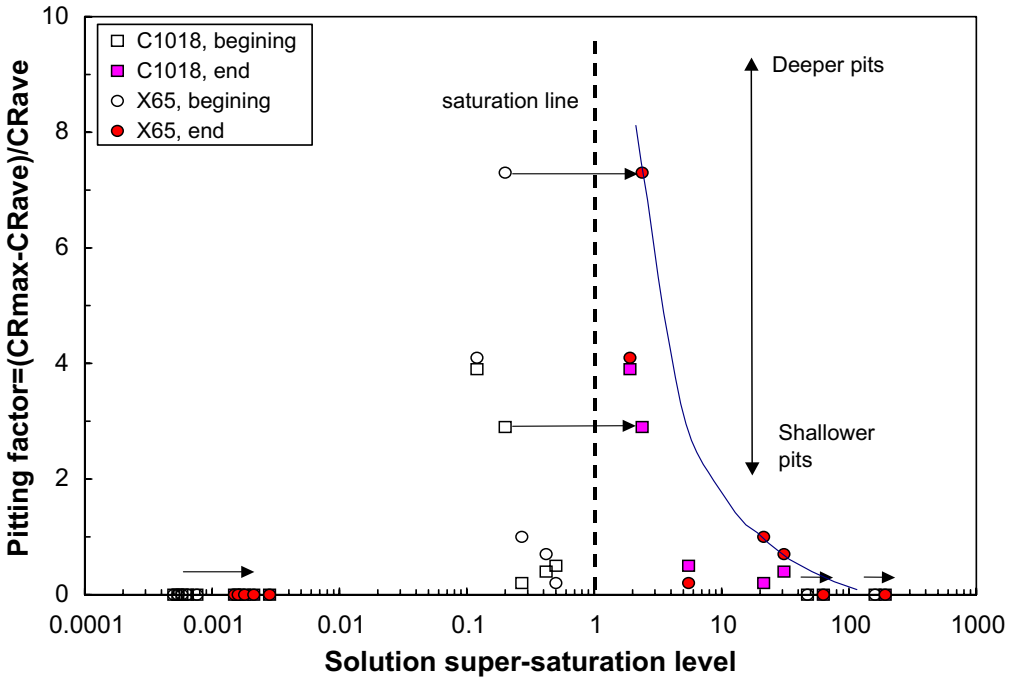

Fig. 12. The effect of iron carbonate supersaturation on localized attack as quantified by the pitting factor showing that the most severe pitting is obtained for relatively small supersaturation when partially protective films are formed. Data taken from long term experiments by Sun and Nešić [43], where the open symbols denote supersaturation at the beginning of the experiments and red-filled symbols denote end of experiments.

into the grey zone, making this sound like a difficult proposal to model. However, it has recently been shown that there is a single parameter such as supersaturation that can successfully describe this behaviour. Sun and Nešić [43] proved experimentally that supersaturation can be used as a good predictor of the probability for localized attack (see Fig. 12). This approach has recently been integrated into the existing quantitative CO_2 corrosion prediction models [21].

Based on mostly anecdotal evidence (field experience), the presence of H_2S and HAc was related to onset of localized attack, however little is understood about how and when this may happen.

3. The mathematical models

Many different mathematical models for CO_2 corrosion are used nowadays by engineers in the oil and gas industry. Some are described in the open literature, others are proprietary models. The latter are typically a variation of publicly available models or are dubious empirical correlations based on practical experience. Nyborg [45] has recently reviewed the performance of a representative sample of CO_2 corrosion prediction models by comparing them to a field database. Complementing that performance-based review, the present review focuses on the different strategies the predictive models employ to account for the complex processes underlying CO_2 corrosion. Indeed, insightful comments could here be made only about those models where there is sufficient information in the public domain, limiting the present review primarily to the models described in the open literature.

In order to classify the CO_2 corrosion models they have arbitrarily been grouped into three broad categories based on how firmly they are grounded in theory.

Mechanistic models: these models describe the mechanisms of the underlying reactions and have a strong theoretical background. Most of the constants appearing in this type of models have a clear physical meaning. Many of the constants are easily found in the literature, while some have still to be obtained by comparing the predictions with available experiments. When calibrated with a reliable (and not necessarily large) experimental database this type of models enable accurate and physically realistic *interpolation* (prediction within the bounds of calibrating parameters), as well as good *extrapolation* predictions. It is easy to add new knowledge to these models with minimal modification of the existing model structure and without having to recalibrate all the model constants.

Semi-empirical models: these models are only partly based on firm theoretical hypotheses. They are for practical purposes extended to areas where insufficient theoretical knowledge is available in a way that the additional phenomena are described with empirical functions. Some of the constants appearing in these models have a clear physical meaning while others are arbitrary best-fit parameters. Calibrated with a sufficiently large and reliable experimental database these models can enable good interpolation predictions. However, extrapolation can lead to unreliable and sometimes physically unrealistic results. New knowledge can be added with moderate effort usually by adding correction factors and/or by doing a partial recalibration of the model constants.

Empirical models: these models have very little or no theoretical background. Most constants used in them have no physical meaning – they are just best-fit parameters to the available experimental results. When calibrated with a very large and reliable experimental database, these models can give good interpolation. However, any extrapolation leads to unreliable results as there are no assurances that the arbitrary empirical correlations hold outside their calibration domain. Addition of any new knowledge to these models is rather difficult and often requires recalibration of the whole model. Alternatively, correction factors can be added with a large degree of uncertainty related to their interaction with the existing empirical constants.

3.1. Mechanistic models

3.1.1. The beginnings

Since CO_2 corrosion is an electrochemical phenomenon it is not surprising that a number of authors started out with mathematical modelling of corrosion by describing the electrochemical processes occurring at the metal surface. Although there is no dispute about the fact that the surface electrochemistry is an important factor in the overall process, it was and still is argued by sceptics that the rate limiting step is often elsewhere in the process (e.g. in mass transport through a surface scale) and that detailed and often very complex modelling of the electrochemical processes is of limited value.

One of the first and most widely used mechanistic models is the one proposed by de Waard and Milliams [5,46] in 1973. Based on the assumption of direct reduction of H_2CO_3 (as presented previously in the text) and their own glass cell experiments, the authors presented a correlation for the corrosion rate which is a function of the and temperature

$$\log V_{\text{cor}} = 7.96 - \frac{2320}{t + 273} - 5.55 \times 10^{-3} t + 0.67 \log p_{CO_2} \tag{12}$$

The 0.67 factor in front of P_{CO_2} was obtained by assuming that the pH is a function of P_{CO_2} only; that is: all the H^+ ions in solution come from dissociation of carbonic acid. While this assumption holds for pure/condensed water–CO_2 solutions, the presence of other species which are normally present when steel corrodes in brines, means that this is no longer true. The temperature function in (12) was obtained by assuming an Arhenius-type dependence for a charge transfer controlled process. In their derivation, the authors assumed that the anodic process of iron dissolution proceeds via a pH-dependent BDD mechanism [4]. It is known today that this assumption does not hold [3,11,15]. As new experimental data emerged, new model constants were determined [32,33] e.g. from experiments of Dugstad et al. [59] without changing the original "base equation". The scope of de Waard and Milliams [46] model was revised on several occasions [32,33] to extend its validity into areas where protective scales form, to account for high pH in brines, velocity, water wetting, glycol, etc. However, this was done by using correction factors (multipliers to the original Eq. (12)) which violate the assumptions under which the original equation was derived. This necessarily took the original mechanistic modelling strategy into the area of semi-empirical modelling which is discussed in the following section. Despite all the theoretical shortcomings, the model of de Waard and Milliams [46] stood as one of the important reference points for CO_2 corrosion research over the past two decades and in its most recently revised form [33], is still used as an informal industrial standard.

3.1.2. Electrochemical models

Almost two decades later Gray et al. [7,8] presented a more complete electrochemical model as a part of their experimental study of CO_2 mechanisms. A number of mechanisms for the electrochemical reactions occurring at the metal surface were adopted from the literature and included into an overall model. The model constants were determined from their own glass cell experiments and flow cell experiments (for higher temperatures). In its scope and approach this was a "breakthrough" study in the field of CO_2 corrosion modelling. The authors ambitiously attempted to cover an unrealistically broad unrealistic range of parameters (e.g. pH 2–11, $t = 25$–125 °C) with a rather simple theoretical framework which inevitably lead oversimplifications and omissions of some key phenomena such as scale formation etc. Despite its undoubted potential, surprisingly few researchers in the field have continued along this theoretical path.

One of the rare follow-up studies is the one by Nešić et al. [15] where the authors also presented an electrochemical model of CO_2 corrosion. Physical constants appearing in the model were determined from the literature, or when missing, found from numerous rotating cylinder glass cell experiments. Most of the experimental observations and physical constants found in this study confirmed the findings of Gray et al. [7,8]. The predictions made with the model were successfully compared with independent pipe-flow glass-loop experiments demonstrating the ability of mechanistic models for extrapolation. The authors also compared their predictions with two other popular models at the time: the semi-empirical models of de Waard et al. [32] and the empirical model of Dugstad et al. [59] (presented below) obtaining reasonable agreement.

In a similar development, Anderko et al. [44] have continued with the electrochemical modelling approach combining it with advanced water chemistry models. Recently George et al. [28] have presented an extension of Nešić et al. [15] electrochemical model which includes the effect of HAc.

In all of the electrochemical models mentioned above the cathodic current i_c is found as:

$$\frac{1}{i_c} = \frac{1}{i_{ct}} + \frac{1}{i_{lim}} \tag{13}$$

where the first term reflects the charge transfer controlled current:

$$i_{ct} = i_o \cdot 10^{-\frac{\eta}{b_c}} \tag{14}$$

while the second term is the limiting current. In the case of H^+ reduction, the limiting current comes from the mass transfer limitation for H^+ reduction:

$$i^d_{lim(H^+)} = k_m F \cdot [H^+]_b \tag{15}$$

and in the case of H_2CO_3 reduction the limiting current is a consequence of a slow CO_2 hydration step and can be found as [47]:

$$i^r_{lim(H_2CO_3)} = F \cdot [CO_2]_b \cdot (D_{H_2CO_3} K_{hyd} k^f_{hyd})^{0.5} \tag{16}$$

Nešić et al. [48] later proposed a theoretical flow multiplier f for this expression which is significantly different from unity only when the thickness of the mass transfer boundary layer is of the same order of magnitude as the reaction layer for H_2CO_3 hydration (at lower temperatures and higher velocities).

$$f = \coth \zeta \tag{17}$$

which takes into account the effect of flow on the chemical reaction limiting current. Parameter ζ is the ratio of the thicknesses of the diffusion and reaction boundary layers.

George et al. [28] have shown that the limiting current for HAc reduction is mass transfer limiting and has the same form as the one for hydrogen ion reduction:

$$i^d_{lim(HAc)} = k_m F [HAc]_b \tag{18}$$

where k_m is the HAc mass transfer coefficient in m/s and $[HAc]_b$ is the bulk concentration of HAc.

For the case of direct H_2O reduction there is no limiting current. For the anodic dissolution of iron pure Tafel behaviour was assumed close to the corrosion potential and the anodic current is:

$$i_a = i_{o(Fe)} \cdot 10^{\frac{\eta}{b_a}} \tag{19}$$

The corrosion potential and current was then found from the equality:

$$\sum i_c = i_a \tag{20}$$

The corrosion rate, CR, can be calculated simply from the anodic (corrosion) current i_a. All the models of this type can be criticised on the grounds that while they described in detail the electrochemical processes occurring on the metal surface, the treatment of the transport processes and chemical processes in the boundary layer was oversimplified. This is particularly important when a reliable prediction of protective scale formation is sought. Therefore a new generation of corrosion models emerged where the transport and the chemical aspects of CO_2 corrosion were improved.

3.1.3. Transport based electrochemical models

Turgoose et al. [49] were the first to pave the way for a more realistic way of describing the transport processes in the boundary layer for the case of CO_2 corrosion. While they have oversimplified the effect of electrochemical reactions, this was soon rectified in the subsequent studies of Pots [30] and others [21,17]. This new coupled transport/electrochemical approach is long established in other areas of electrochemistry [50] and crevice corrosion [51], and its essential logic is briefly described below for the case of CO_2 corrosion.

In corrosion, certain species in the solution are "produced" at the steel surface (e.g. Fe^{2+}) while others are depleted (e.g. H^{+}) by the electrochemical reactions. This leads to concentration gradients and diffusion of these species towards and away from the surface. The concentration of each species is governed by a species conservation (mass balance) equation. A universal one-dimensional form of the equation which describes transport for species j in the presence of chemical reactions, which is valid both for the liquid boundary layer and the porous scale, is:

$$\underbrace{\frac{\partial(\varepsilon c_j)}{\partial t}}_{\text{accumulation}} = \underbrace{\frac{\partial}{\partial x}\left(\varepsilon^{1.5} D_j^{\text{eff}} \frac{\partial c_j}{\partial x}\right)}_{\text{net flux}} + \underbrace{\varepsilon R_j}_{\text{source or sink due to chemical reactions}} \tag{21}$$

Turbulent convection is approximated by *turbulent diffusion* as the former is difficult to determine explicitly. Electromigration has been neglected as its contribution to the overall flux of species in free corrosion is small.

One transport equation of the form (21) can be written for each species in the solution (for a list see Table 1). The resulting set of equations is solved simultaneously in space and time. The boundary conditions for this set of partial differential equations are:

- *at the steel surface*: flux of species as determined from the rate of the electrochemical reactions given by Eqs. (14) and (19);
- *in the bulk* : equilibrium concentrations of species as obtained by solving the set of equilibria listed in Table 2.

As the transport equation (21) is transient, initial conditions need to be defined. Typically a bare metal surface with the solution in chemical equilibrium is used as the initial condition. The modelling can be done with different initial conditions such as steel surface covered with a pre-existing mill scale, etc.

Once the set of equations is solved for any given time step, the corrosion rate, CR, can be simply calculated as the flux of Fe^{2+} ions at the metal surface.

A variety of chemical reactions accompanies the CO_2 corrosion process. By affecting the surface concentrations of species, chemical reactions can significantly alter the rate of electrochemical processes at the steel surface and the rate of corrosion. This is particularly true when, due to high local concentrations of species, the solubility limit is exceeded and precipitation of surface scales occurs.

The rate of a homogeneous chemical reaction (shown in Table 2) can be calculated, assuming ideal solutions, as:

$$R_j = k_{\text{f}} \prod_{r=1}^{n_r} c_r - k_{\text{b}} \prod_{p=1}^{n_p} c_p \tag{22}$$

The rate of precipitation of iron carbonate $R_{FeCO_{3(s)}}$ can be described as:

$$R_{FeCO_{3(s)}} = \frac{A}{V} \cdot f(T) \cdot K_{sp} \cdot f(S) \tag{23}$$

Supersaturation is defined as:

$$S = \frac{c_{Fe^{2+}} c_{CO_3^{2-}}}{K_{sp}} \tag{24}$$

The kinetic expression for iron carbonate precipitation as proposed by Johnson and Tomson [52] or Van Hunnik et al. [42] can be used here for $f(S)$. Iron carbonate scale growth depends primarily on the precipitation rate, R_{FeCO_3} as well as the rate of undermining governed by the corrosion rate. This can be expressed as a mass balance equation for solid iron carbonate in terms of the volumetric scale porosity ε:

$$\underbrace{\frac{\partial \varepsilon}{\partial t}}_{\text{film porosity change}} = \underbrace{-\frac{M_{FeCO_{3(s)}}}{\rho_{FeCO_{3(s)}}} R_{FeCO_{3(s)}}}_{\text{precipitation}} - \underbrace{CR \frac{\partial \varepsilon}{\partial x}}_{\text{undermining}} \tag{25}$$

Solution of this equation simultaneously with the transport equation (21) and the electrochemical equation (20) enables direct calculations of porosity, thickness as well as the protective properties of iron carbonate scales. For more details see Nešić at al. [53].

Other simpler variations of transport based models of CO_2 corrosion exist. For example Dalayan et al. [54,55] used a mass transfer coefficient for straight pipe flow instead of the transport equation (21) and neglected the kinetics of chemical reactions. Achour et al. [56] have used a similar model to simulate pit propagation of carbon steel in CO_2 environments under highly turbulent conditions.

The transport based models outlined above can be readily and logically linked to flow models and in particular multiphase flow models. One of the more complete attempts was recently presented by Nešić et al. [21]. They have presented an integrated CO_2 corrosion/multiphase flow model where mechanistic methods were described for predicting various flow regimes (e.g. slug, stratified, annular) as well as the for calculating key hydrodynamic parameters in multiphase flow such as water layer thickness and velocity, wall shear stress, slug frequency, etc. However, the most significant effect of multiphase flow on corrosion in oil and gas pipelines is related to water wetting/entrainment. Rules of thumb or empirical functions were used in the past (discussed in the section below). The new model of Nešić et al. [21] builds on a well established hydrodynamic theory of Brauner [57] and Barnea [58]. A criterion for forming stable water-in-oil dispersed flow was derived as the means of calculating the critical velocity for water entrainment within the liquid layer. Two main physical properties, *maximum droplet size* related to break-up and coalescence and *critical droplet size* related to settling and separation, were compared to deduce this criterion.

3.2. Semi-empirical models

By far the most commonly used and the best-known model of CO_2 corrosion is the semi-empirical model of de Waard and collaborators [32,33]. Following the initial landmark study [5] which resulted in a mechanistic model, de Waard made "improvements" to the original model mostly by recalibrating the model constants against the emerging, more reliable, experiments (e.g. Dugstad et al. [59]) and by adding numerous correction

factors to the original correlation (12), to account for various complicating effects as discussed below. Other semi-empirical models can be found in the literature [60,61]. However, they can be seen most often as variations of the de Waard models, where the experimental database is different, and the curve fitting strategy is more or less advanced.

In the work of de Waard and Lotz [32] the effect of velocity in the absence of surface scales was modelled via a *parallel resistance* model:

$$\frac{1}{V_{\mathrm{cor}}} = \frac{1}{V_{\mathrm{r}}} + \frac{1}{V_{\mathrm{m}}} \tag{26}$$

where the first term on the right hand side represents the rate of electrochemical processes, while the second denotes mass transfer. It is interesting that this equation which is proposed following a simple electrical circuit analogy actually resembles the cathodic Eq. (13) which is derived directly from electrochemical theory. This explains the success which the resistance model had in approximating the experimental results, compared with the original Eq. (12) which did not include any provisions for the effect of velocity.

As the original Eq. (12) was derived exclusively for pure/condensed water (low pH) water, a correction which accounts for the effect of pH was added along with a correction factor for protective scales [32]. The latter was obtained by doing a multi-dimensional regression on the high temperature CO_2 corrosion experiments of Ikeda et al. [62]. The problem with this approach is that the initial theoretical correlation (12) which was being "corrected" is valid only under pure charge transfer control conditions. Presence of protective scales often implies mass transfer control of the corrosion process – thus rendering the previous charge-transfer based correlation invalid.

In the work of de Waard and Lotz [32] the presence of the oil phase was accounted for through a so-called water-wetting factor. From the original experiments of Wicks and Fraser [63], a binary prediction factor was extracted suggesting that oil-wetting will occur only for water cuts (contents) less than 30% *and* velocities larger than 1 m/s when all water can be entrained in the oil phase. This is a crude criterion that neglects many key factors such as: the properties of the oil and water phases, the flow regime and the flow geometry. Furthermore, field experience suggests that in some cases corrosion was obtained at water cuts as low as 2%, in others no corrosion was obtained for water cuts as high as 50%.

de Waard et al. [64] in 2001 and 2003 updated the original de Waard and Lotz [32] empirical correction factor for water wetting from 1993 and proposed a new empirical factor using an analysis based on the emulsion breakpoint approach. A link between API gravity, emulsion stability and water wetting of steel by an oil–water mixture was considered by taking into account the changes in interfacial tensions in an oil–water–steel system. This was a major step forward from the original model, however, while agreeing reasonably well with the specific pool of field cases used for its calibration, the new model remained an empirical correlation built on limited field data with an uncertain potential for extrapolation. More importantly, this model does not consider the effect of pipe diameter, oil density, oil viscosity and system temperature on the critical velocity of the flowing oil phase required for entrainment.

3.3. Empirical models

One of the most frequently encountered empirical models is the one by Dugstad et al. [59] which is based on the same experimental database as the model of de Waard et al. [33].

The initial approach of Dugstad et al. [59] was to determine a temperature-dependent "basic equation" (a best-fit polynomial function) and then multiply it by the correction factors for p_{CO_2}, pH, velocity (shear stress) and steel Cr content. The basic equation has a maximum in the high temperature range, mimicking the protective effect of iron carbonate protective scales. The correction factor for flow was defined as a combined power-law/exponential function of the wall-shear stress, an approach similar to Efird et al. [60]. The pH and p_{CO_2} correction factors resemble those used by de Waard and Lotz [32]. This simple empirical model is at the core of the so-called NORSOK model which has been uncritically and widely used due to the fact that it is "standardized" and freely available at http://www.standard.no.

Another example of an empirical CO_2 corrosion model is the linear multiple regression model shown by Adams et al. [65]. It is doubtful that a linear model (even if it is multivariable) can describe well the highly nonlinear processes occurring in CO_2 corrosion.

More recently, Nešić et al. [66] have presented a highly nonlinear empirical CO_2 corrosion model based on neural networks (NN) using the experimental database of Dugstad et al. [59] for calibration. The correlation was developed by using a "back propagation" neural network combined with a genetic algorithm [67,68]. Generally, neural networks are aimed for prediction or pattern recognition problems, for which it is difficult to develop a suitable analytical model. During the training, the network operates interactively with a genetic algorithm. Genetic algorithms are stochastic search tools for determination of the fittest problem solution according to some pre-defined criteria. The purpose of the genetic algorithm, is to accelerate the network training by determination of the most representative sequence of training patterns from the training data set. The fittest training sequence generates the minimal training error. The NN model demonstrated superior performance when calibrated with the Dugstad et al. [59] database when compared to the empirical model of Dugstad et al. [59], the semi-empirical model of de Waard et al. [33] and the mechanistic electrochemical model of Nešić et al. [15].

Despite this apparent advantage over other types of modelling, the key problem with the NN and other fully empirical models is that they are "black boxes" i.e. their prediction algorithms, being arbitrary mathematical functions, offer virtually no meaningful insight into the nature of the predictions they offer and therefore they cannot be used with confidence outside their calibration range (for extrapolation). Adding new knowledge is tedious and usually requires recalibration of the entire model with all the data.

4. Conclusions

Understanding internal corrosion in oil and gas pipelines made from carbon steel (CO_2 corrosion) has come a long way over the past few decades. The influence of the many important electrochemical, chemical, hydrodynamic and metallurgical parameters has been uncovered, with some major challenges lying ahead.

- Electrochemistry of mild steel dissolution in CO_2 solutions has largely been understood and modelled, with the outstanding issues primarily related to other environments (H_2S and HAc, inhibitors) and different steels.
- Key mechanisms leading to formation of iron carbonate scales have been identified. Scaling tendency is identified as the parameter that effectively describes how the competition of precipitation and corrosion can lead to both protective and unprotective sur-

face scales. The effect of other types of scales/scales such as calcium carbonate, etc. is still largely unknown.

- The effect of pH on CO_2 corrosion is well established and successfully modelled, both at low pH typical for condensed water as well as higher pH when protective scales form. In almost all cases higher pH leads to lower corrosion rates.
- The presence of organic acids and their effect on CO_2 corrosion is an issue that was largely ignored until recently. However, major advancements in understanding of the role of HAc have been made in the past few years with a few open issues remaining, primarily related to the effect of HAc on localized attack.
- The effect of temperature, which is well known to accelerate all processes involved in CO_2 corrosion, has been clarified. At low pH when protective scales do not form, temperature accelerates corrosion and vice versa when conditions are favourable for iron carbonate to form, temperature leads to faster precipitation and often to lower corrosion rates.
- A way has been charted to account for the effect of flow and in particular multiphase flow on CO_2 corrosion. The most important effect related to water wetting/entrainment is now understood from a hydrodynamic point of view. The effect of violent slug flow on protective scale/inhibitor removal needs further investigation.
- It has been shown that various mild steels have approximately the same behaviour when it comes to scale-free CO_2 corrosion. The effect on protective scale formation as well as inhibitor performance is an open issue.
- Problems related to prediction of corrosion control by inhibition remain, particularly when it comes to the performance of inhibitors in slug flow, in the presence of surface scales/scales, H_2S or HAc.
- Systematic work on understanding of the effect on CO_2 corrosion of inhibitors present in the crude oil has been initiated, with a more dedicated follow-up needed that will cover a broader range of crude oils.
- Understanding of the effect of water condensation leading to Top-of-Line-Corrosion (TLC) attack was advanced significantly over the past decade. Remaining challenges relate to the effect of HAc, H_2S as well as effective mitigation techniques.
- Only rudimentary understanding of the effect of glycol/methanol on CO_2 corrosion exists. More fundamental work is needed before any meaningful modelling can be achieved.
- Localized attack, being the most dangerous type of CO_2 corrosion attack is still difficult to predict. While many factors ranging from metallurgical, hydrodynamic to (electro)chemical can influence the onset of localized corrosion, it appears that much of the evidence points towards existence of a "grey zone" where localized attack is more likely to occur. The "grey zone" seems to be associated with the formation of partially protective scales.
- Various mathematical modelling strategies can be used to capture our understanding of CO_2 corrosion.
  - *Mechanistic models* are the most direct translation of our knowledge of the underlying processes into mathematical functions. They are the hardest ones to construct and have the largest potential to help engineers in various stages of the design, operations and control operations.
  - *Semi-empirical models*, which have a limited amount of inbuilt understanding, rely on correction factors to perform well. These factors come in the form of arbitrary

functions developed on sparse experimental databases and have dubious interactions. While being significantly easier to develop than mechanistic models, the capability of semi-empirical models to extrapolate is questionable.

– *Empirical models* consisting of arbitrary mathematical functions of varying complexity, can have reasonable or even excellent interpolation capabilities but have to be treated with utmost caution when used to predict outside they calibration range.

References

[1] D.M. Drazic, Iron and its electrochemistry in an active state, Aspects of Electrochemistry, vol. 19, Plenum Press, 1989, p. 79.
[2] W. Lorenz, K. Heusler, Anodic dissolution of iron group metals, in: F. Mansfeld (Ed.), Corrosion Mechanisms, Marcel Dekker, New York, 1987.
[3] S. Nešić, N. Thevenot, J.L. Crolet, Electrochemical properties of iron dissolution in CO_2 solutions – basics revisited, Corrosion/96, paper no. 3, (Houston, TX: NACE International, 1996).
[4] J.O.M. Bockris, D. Drazic, A.R. Despic, Electrochim. Acta 4 (1961) 325.
[5] C. de Waard, D.E. Milliams, Corrosion 31 (1975) 131.
[6] G. Schmitt, B. Rothman, Werkst. Korros. 28 (1977) 816.
[7] L.G.S. Gray, B.G. Anderson, M.J. Danysh, P.G. Tremaine, Mechanism of carbon steel corrosion in brines containing dissolved carbon dioxide at pH 4, Corrosion/89, paper no. 464 (Houston, TX: NACE International, 1989).
[8] L.G.S. Gray, B.G. Anderson, M.J. Danysh, P.R. Tremaine, Effect of pH and temperature on the mechanism of carbon steel corrosion by aqueous carbon dioxide, Corrosion/90, paper no. 40 (Houston, TX: NACE International, 1990).
[9] T. Hurlen, S. Gunvaldsen, R. Tunold, F. Blaker, P.G. Lunde, J. Electroanal. Chem. 180 (1984) 511.
[10] H. Davies, G.T. Burstein, Corrosion 36 (1980) 385.
[11] K. Videm, Fundamental studies aimed at improving models for prediction of CO_2 corrosion, in: Proceedings from 10th European Corrosion Congress, Progress in the Understanding and Prevention of Corrosion, vol. 1, Institute of Metals, London, 1993, p. 513.
[12] E. Eriksrud, T. Søntvedt, Effect of flow on CO_2 corrosion rates in real and synthetic formation waters, advances in CO_2 corrosion, in: R.H. Hausler, H.P. Goddard (Eds.), Proceedings of the Corrosion/83 Symposium on CO_2 Corrosion in the Oil and Gas Industry, vol. 1, NACE, Houston, TX, 1984, p. 20.
[13] M.R. Bonis, J.L. Crolet, Basics of the prediction of the risks of CO_2 corrosion in oil and gas wells, Corrosion/89, paper no. 466 (Houston, TX: NACE International, 1989).
[14] P. Delahay, J. Am. Chem. Soc. 74 (1952) 3497.
[15] S. Nešić, J. Postlethwaite, S. Olsen, An electrochemical model for prediction of CO_2 Corrosion, Corrosion/95, paper no. 131 (Houston, TX: NACE International, 1995).
[16] S. Nešić, M. Nordsveen, R. Nyborg, A. Stangeland, A mechanistic model for CO_2 corrosion of mild steel in the presence of protective iron carbonate scales – Part II: A numerical experiment, Corrosion 59 (2003) 489.
[17] M. Nordsveen, S. Nešić, R. Nyborg, A. Stangeland, A mechanistic model for carbon dioxide corrosion of mild steel in the presence of protective iron carbonate scales – Part 1: Theory and verification, Corrosion 59 (2003) 443.
[18] K. Chokshi, W. Sun, S. Nešić, Iron carbonate film growth and the effect of inhibition in CO_2 corrosion of mild steel, Corrosion/05, paper no. 285 (Houston, TX: NACE International, 2005).
[21] S. Nešić, S. Wang, J. Cai, Y. Xiao, Integrated CO_2 corrosion – multiphase flow model, Corrosion/04, paper no. 626 (Houston, TX: NACE International, 2004).
[22] Y.M. Gunaltun, D. Larrey, Correlation of cases of top of line corrosion with calculated water condensation rates, CORROSION/2000, paper no. 71 (Houston, TX: NACE International 2000).
[23] B. Hedges, L. McVeigh, The role of acetate in CO_2 corrosion: The double whammy CORROSION/1999, paper no. 21 (Houston TX: NACE International 1999).
[24] Y. Garsany, D. Pletcher, B. Hedges, The role of acetate in CO_2 corrosion of carbon steel: has the chemistry been forgotten? CORROSION/2002, paper no. 2273 (Houston, TX: NACE International, 2002).
[25] Y. Sun, K. George, S. Nešić, The effect of Cl- and acetic acid on localized CO_2 corrosion in wet gas flow, CORROSION/2003, paper no. 3327, (Houston, TX: NACE International 2003).

[26] S. Wang, K. George, S. Nešić, High pressure CO_2 corrosion electrochemistry and the effect of acetic acid, CORROSION/2004, paper no. 375 (Houston, TX: NACE International, 2004).
[27] K. George, S. Wang, S. Nešić, C. de Waard, Modeling of CO_2 corrosion of mild steel at high partial pressures of CO_2 and in the presence of acetic acid, CORROSION/2004, paper no. 623 (Houston, TX: NACE International, 2004).
[28] K. George, S. Nešić, C. de Waard, Electrochemical investigation and modeling of CO_2 corrosion of mild steel in the presence of acetic acid, CORROSION/2004, paper no. 379 (Houston, TX: NACE International, 2004).
[29] O.A. Nafday, S. Nešić, Iron carbonate film formation and CO_2 corrosion in the presence of acetic acid, CORROSION/2005, paper no. 295 (Houston, TX: NACE International, 2005).
[30] B.F.M. Pots, Mechanistic models for the prediction of CO_2 corrosion rates under multiphase flow conditions, Corrosion/95, paper no. 137 (Houston, TX: NACE International, 1995).
[31] W.P. Jepson, C. Kang, M. Gopal, S. Stitzel, Model for sweet corrosion in horizontal multiphase slug flow, CORROSION/97, paper no. 11, (Houston Texas: NACE International, 1997).
[32] C. de Waard, U. Lotz, Prediction of CO_2 corrosion of carbon steel, Corrosion/93, paper no. 69 (Houston, TX: NACE International, 1993).
[33] C. de Waard, U. Lotz, A. Dugstad, Influence of liquid flow velocity on CO_2 corrosion a semi-empirical model, Corrosion/95, paper no. 128 (Houston, TX: NACE International, 1995).
[34] S. Nešić, W. Wilhelmsen, S. Skjerve, S.M. Hesjevik, Testing of inhibitors for CO_2 corrosion using the electrochemical techniques, in: Proceedings of the 8th European Symposium on Corrosion Inhibitors, Ann. Univ. Ferrara, N.S., Sez. V, Suppl. N. 10, 1995.
[35] C. Mendez, S. Duplat, S. Hernandez, J. Vera, On the mechanism of corrosion inhibition by crude oils, CORROSION/2001, paper no. 44 (Houston, TX: NACE International, 2001).
[36] S. Hernandez, S. Duplat, J. Vera, E. Baron, A statistical approach for analyzing the inhibiting effect of different types of crude oil in CO_2 corrosion of carbon steel, CORROSION/2001, paper no. 293 (Houston, TX: NACE International, 2002).
[37] S. Hernandez, J. Bruzual, F. Lopez-Linares, J. Luzon, Isolation of potential corrosion inhibiting compounds in crude oils, CORROSION/2003, paper no. 330 (Houston, TX: NACE International, 2003).
[38] J. Cai, S. Nešić, C. de Waard, Modeling of water wetting in oil–water pipe flow, CORROSION/2004, paper no. 663 (Houston, TX: NACE International, 2003).
[39] F. Vitse, S. Nešić, Y. Gunaltun, D. Larrey de Torreben, P. Duchet-Suchaux, Mechanistic model for the prediction of top-of-the-line corrosion risk, Corrosion 59 (2003) 1075.
[40] Y.M. Gunaltun. Combining research and field data for corrosion rate prediction, CORROSION/96, paper no. 27 (Houston Texas: NACE International, 1996).
[41] G. Schmitt, C. Bosch, M. Mueller, G. Siegmund, CORROSION/ 2000, paper no. 49, NACE International, Houston, Texas, 2000.
[42] E.W.J. van Hunnik, B.F.M. Pots, E.L.J.A. Hendriksen, The formation of protective $FeCO_3$ corrosion product layers in CO_2 corrosion, CORROSION/96, paper no. 6 (Houston, TX: NACE International, 1996).
[43] Y. Sun, S. Nešić, A parametric study and modeling on localized CO_2 corrosion in horizontal wet gas flow, CORROSION/2004, paper no. 380 (Houston, TX: NACE International, 2004).
[44] A. Anderko, R. Young, Simulation of CO_2/H_2S corrosion using thermodynamic and electrochemical models, CORROSION/99, paper no. 31 (Houston, TX: NACE International, 1999).
[45] R. Nyborg, Overview of CO_2 corrosion models for wells and pipelines, CORROSION/2002, paper no. 233 (Houston, TX: NACE International, 2002).
[46] C. de Waard, D.E. Milliams, Prediction of carbonic acid corrosion in natural gas pipelines, in: First International Conference on the Internal and External Corrosion of Pipes, paper F1, University of Durham, UK, 1975.
[47] K.J. Vetter, Electrochemical Kinetics, Theoretical Aspects, Sections 1, 2, and 3 of Electrochemical Kinetics: Theoretical and Experimental Aspects, translation from German, Academic Press, New York, 1967, p. 235.
[48] S. Nešić, B.F.M. Pots, J. Postlethwaite, N. Thevenot, Superposition of diffusion and chemical reaction limiting currents – application to CO_2 corrosion, Journal of Corrosion Science and Engineering, vol. 1, paper no. 3, World Wide Web. http://www.cp.umist.ac.uk/JCSE/Vol1/PAPER3/V1_p3int.htm, The Corrosion Information Server, The Corrosion & Protection Centre at UMIST, Manchester, UK, 1995.
[49] S. Turgoose, R.A. Cottis, K. Lawson, Modelling of electrode processes and surface chemistry in carbon dioxide containing solutions, in: ASTM Symposium on Computer Modelling of Corrosion, San Antonio, 1990.
[50] J.S. Newman, Electrochemical Systems, Part C, Second ed., Prentice Hall, 1991.

[51] M.K. Watson, J. Postlethwaite, Corrosion 46 (1990) 522.
[52] M.L. Johnson, M.B. Tomson, Ferrous carbonate precipitation kinetics and its impact on CO_2 corrosion, CORROSION/91, paper no. 268 (Houston, TX: NACE International, 1991).
[53] S. Nešić, K.-L.J. Lee, A mechanistic model for CO_2 corrosion of mild steel in the presence of protective iron carbonate scales – Part O: Scale growth model, Corrosion 59 (2003) 616.
[54] E. Dayalan, G. Vani, J.R. Shadley, S.A. Shirazi, E.F. Rybicki, Modelling CO_2 corrosion of carbon steel in pipe flow, Corrosion/95, paper no. 118 (Houston, TX: NACE International, 1995).
[55] E. Dayalan, F.D. de Moraes, J.R. Shadley, S.A. Shirazi, E.F. Ribicki, CO_2 corrosion prediction in pipe flow under $FeCO_3$ scale-forming conditions, CORROSION/98, paper no. 51 (Houston, TX: NACE International, 1998).
[56] M.H. Achour, J. Kolts, A.H. Johannes, G. Liu, Mechanistic modelling of pit propagation in CO_2 environments under high turbulence effects, Corrosion/93, paper no. 87 (Houston, TX: NACE International, 1993).
[57] N. Brauner, The prediction of dispersed flows boundaries in liquid–liquid and gas–liquid systems, Int. J. Multiphase Flow 27 (2001) 885–910.
[58] D. Barnea, A unified model for predicting flow pattern transitions for the whole range of pipe inclinations, Int. J. Multiphase Flow 11 (1987) 1–12.
[59] A. Dugstad, L. Lunde, K. Videm, Parametric study of CO_2 corrosion of carbon steel, Corrosion/94, paper no. 14 (Houston, TX: NACE International, 1994).
[60] K.D. Efird, E.J. Wright, J.A. Boros, T.G. Hailey, Wall shear stress and flow accelerated corrosion of carbon steel in sweet production, in: 12th International Corrosion Congress, paper no. TS 14 194 (Houston, TX: NACE International, 1993).
[61] S. Kanwar, W.P. Jepson, A model to predict sweet corrosion of multiphase flow in horizontal pipelines, Corrosion/94, paper no. 24 (Houston, TX: NACE International, 1994).
[62] A. Ikeda, S. Mukai, M. Ueda, Prevention of CO_2 corrosion of line pipe and oil country tubular goods, Corrosion/84, paper no. 289 (Houston, TX: NACE International, 1984).
[63] M. Wicks, J.P. Fraser, Mater. Perform. 14 (May) (1975) 9.
[64] C. de Waard, L. Smith, B.D. Craig, The influent of crude oil on well tubing corrosion rates, EUROCORR, 2001.
[65] C.D. Adams, J.D. Garber, F.H. Walters, C. Singh, Verification of computer modelled tubing life predictions by field data, Corrosion/93, paper no. 82 (Houston, TX: NACE International, 1993).
[66] S. Nešić, J. Postlethwaite, M. Vrhovac, CO2 corrosion of steel: from mechanistic to empirical modelling – a review, Journal of Corrosion Reviews (Special Issue on Application of Computers in Corrosion) XV (1/2) (1997) 211.
[67] M. Vrhovac, Combined empirical and analytical modelling of hardness softening due to particle coarsening using artificial intelligence tools, in: ASME 95 Congress, IMECE Proceedings, MD-Vol. 69-2, San Francisco, California, USA, November 12–17, 1995.
[68] M. Vrhovac, C.R. João and R. Rodrigues, Automation of microstructure analysis by artificial intelligence image processing, in: Int. Conf. SMIRT 13, Post Conference Seminar: Applications of Intelligent Software Systems in Power Plant, Process Plant and Structural Engineering, São Paolo, Brasil, August 21–23, 1995.
[69] S. Nešić, G.T. Solvi, J. Enerhaug, Corrosion 51 (1995) 773.
[70] K-L.J. Lee, S. Nešić, The effect of trace amount of H_2S on CO_2 corrosion investigated by using the EIS technique, Corrosion/05, paper no. 630 (Houston, TX: NACE International, 2005).